UNIVERSITÀ DEGLI STUDI DI TORINO

Department of Clinical and Biological Sciences

PhD Programme in Experimental Medicine and Therapy

Cycle: XXXIII

Dihydroorotate dehydrogenase inhibition reveals metabolic vulnerability in chronic myeloid leukemia

Student: **Mohammad Houshmand**

Tutor: **Prof. Giuseppe Saglio**

PhD program coordinator: **Prof. Pasquale Pagliaro**

Academic year: **2017-2021**

SCIENTIFIC-DISCIPLINARY SECTOR OF AFFERENCE: **MED/15**

GLOSSARY

ITALIAN	ENGLISH
Dipartimento di Scienze Cliniche e Biologiche	Department of Clinical and Biological Sciences
Dottorato di ricerca in Medicina e Terapia Sperimentale	PhD Programme in Experimental Medicine and Therapy
Ciclo XXXIII	Cycle XXXIII
L'inibizione dell' enzima diidroorotato deidrogenasi evidenzio vulnerabilità metabolica nella leucemia mieloide cronica	Dihydroorotate dehydrogenase inhibition reveals metabolic vulnerability in chronic myeloid leukemia
Tesi presentata da Mohammad Houshmand	Thesis' author Mohammad Houshmand
Tutor Prof Giuseppe Saglio	Supervisor Prof. Giuseppe Saglio
Coordinatore del Dottorato prof. Pasquale Pagliaro	PhD Programme Co-ordinator Pasquale Pagliaro
Anni Accademici 2017-2021	Academic years of enrolment 2017-2021
Settore Scientifico Disciplinare di Afferenza MED/15	Code of scientific discipline MED/15

Abstract

Chronic myeloid leukemia is a hematopoietic stem cell disorder emanating from a reciprocal translocation between BCR on chromosome 22 and ABL1 on chromosome 9. The resultant fusion protein through constant tyrosine kinase activity triggers downstream signaling pathways and leads to expansion of leukemic cells.

The development of different generations of BCR/ABL1 tyrosine kinases inhibitors (TKIs) has led the overall survival (OS) of the chronic myeloid leukemia (CML) patients to become almost similar to that of a control population without leukemia, but the TKI therapy can be successfully discontinued only in half of those who are achieving a deep molecular response, that means in approximately 15-20% of the entire population. In addition, although few, there are CML patients who show resistance to TKI therapy, are prone to progress to more advanced phases of the disease, and die of CML-related causes. Therefore, using an alternative approach for the elimination of TKIs resistant leukemic cells is of the essence in trying to solve these problems. It is worth mentioning that BCR/ABL transcript is also detectable in some healthy people. This might confirm that BCR/ABL should be present in a cell that has the biological potential to cause leukemia. So, targeting the metabolic difference between normal and leukemic cells could be a viable option to increase treatment outcomes in CML patients.

Dihydroorotate dehydrogenase (DHODH) is a druggable enzyme in the fourth step of the de novo pyrimidine biosynthesis pathway that is located in the inner membrane of mitochondria. This enzyme catalyzes the oxidation of dihydroorotate to orotate and uses ubiquinone as an electron acceptor.

Here, we found that newly diagnosed and resistant CML CD34+ cells and CML cell lines are sensitive to DHODH inhibition mediated by Meds433, a new and potent DHODH inhibitor recently developed by our group. Meds433 significantly activated the apoptotic pathway and induced cell cycle and cell growth arrest in CML CD34+ cells. Based on the RNA seq analysis, DHODH inhibition enhanced tumor suppressors such as P53 and DDIT3 and reduced oncogenes such as MYC. Also, a decrease in erythroid-related genes and inflammatory profile was recorded. Moreover, based on the metabolic analysis inhibition of DHODH led to the reduction of amino acids and induction of metabolic stress in CML CD34+ cells. Meanwhile, administration of Meds433 10mg/kg and 20mg/kg significantly reduced tumor growth and tumor burden in vivo.

Altogether, our study shows that targeting pyrimidine synthesis is a promising approach for targeting CML 4 stem/progenitor cells, helping more patients to achieve good molecular response and possibly successful treatment discontinuation.

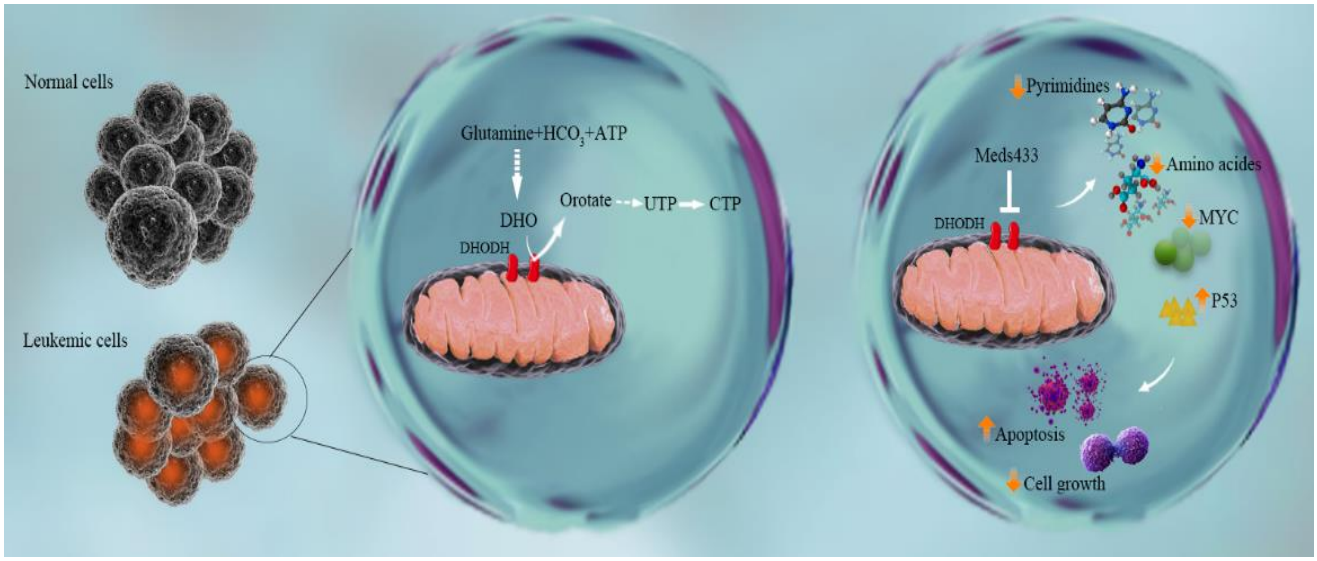

Contents

1-Introduction

1.1- Chronic myeloid leukemia

Chronic myeloid leukemia (CML) is a hematopoietic stem cells disorder emanating from t(9;22) (q34;q11) that results in the proximity of Abelson murine leukemia virus (ABL1) on chromosome 9 and breakpoint cluster region (BCR) on chromosome 22 in a cell with the biological potential to cause leukemia. The encoded protein by constant tyrosine kinase activity triggers downstream signaling pathways and leads to a high proliferation rate and an anti-apoptotic effect. These signaling activities also shift the cells toward myeloid lineage in which a dramatic increase in granulocyte lineage is visible. The incidence rate of CML is about 1-2 in 100000 populations with a male predominance. In western countries, CML is mostly seen in elderly people but in developing countries, it might be seen in the younger population. Historically, CML is divided into three phases including chronic, accelerated, and blastic phases. However most newly diagnosed patients are in the chronic phase with the common presentations of weight loss, night sweat, fatigue, and splenomegaly. Bone marrow is hypercellular with an increase in myeloid to erythroid ratio and the percentage of the blast is usually less than 5% (1, 2).

1.2- Tyrosine kinase inhibitors

Monotherapy with Tyrosine kinase inhibitors (TKIs) is considered the standard of care for the treatment of CML. First-generation of TKIs called imatinib revolutionized treatment outcomes and turned a fatal disease into a controllable one with high overall survival in patients. Imatinib binds inactive BCR/ABL1 and occupies ATP binding site that is mandatory for the conformational change and the kinase activity. Also, it inhibits other TKs such as PDGFRB, c-FMS, ABL2, ABL1, and c-KIT (3). However, about 40-

50% of patients who receive imatinib as the first line of therapy show resistance or intolerance (4). Nilotinib as the second generation of TKIs has shown to be a potent agent in treating nonresponding patients to imatinib (5). Except for BCR/ABL1, it also targets c-KIT and PDGFR (5). In a clinical trial, CML patients were divided into 3 groups; 400mg nilotinib once daily, 300mg nilotinib twice daily, and 400mg imatinib once daily. After 12 months, patients who received nilotinib demonstrated a higher major molecular response (MMR) compared to imatinib (6). Dasatinib another second generation of TKIs has a higher potency compared to imatinib (about 325-fold higher potency) and can bind BCR/ABL1 active form (5, 7, 8). In different clinical trials administration of dasatinib resulted in higher MMR compared to imatinib, though no difference was reported in terms of overall survival and progression-free survival (9, 10). Bosutinib is another second generation TKIs that was first developed as an inhibitor of SRC but then found to be effective against BCR/ABL1 (11, 12). In a clinical trial phase 3, 400mg/daily of bosutinib demonstrated a higher MMR rate in patients compared to imatinib (13). Its lower dose and higher efficacy have led to the approval of bosutinib as a frontline treatment by FDA in 2017. Ponatinib is the third generation of TKIs designed to overcome T315I mutation in which previous TKIs did not show any efficacy against it (5, 14). A phase 3 trial (EPIC) that compared ponatinib 45mg/daily to imatinib 500mg in newly diagnosed patients, was terminated to due the high rate of myocardial infarction, vascular disease, and stroke (15, 16). Considering this, ponatinib might not be suitable for patients with a background of vascular events.

1.3- Treatment free remission

In 2004, some reports claimed that in CML patients who received, TKIs therapy can be discontinued without disease recurrence. Two clinical trials of STIM and TWISTER confirmed that TKIs discontinuation in some patients is feasible without leukemia

recurrence. In these studies, patients with a complete molecular response with 4.5 log reduction in BCR/ABL1 transcript that was under TKIs therapy for more than two years were eligible to stop the therapy in a term called treatment free remission. Following TKIs discontinuation relapse may occur in the first 12 months and therapy needs to be reinitiated. Based on a metadata analysis from 15 different studies, the overall rate of relapse was about 50% and the relapse rate after 6 months was about 41%. The cells results in early relapse might be related to leukemic stem cells (LSCs) that are insensitive to TKIs. These cells that use both BCR/ABL dependent and independent mechanism resides in the same microenvironment as normal HSCs. Previous reports proved the presence of these LSCs in diagnosis, during the treatment, and in patients who are in TFR. This also suggests that we might have a disease recurrence in most patients if we have a long-term follow-up. Apart from disease relapse in patients who are in TFR, some patients are TKIs insensitive from the beginning (17-19).

1.4- TKIs resistance

Patients who respond to TKIs therapy have a life expectancy almost similar to healthy people. However, TKIs resistance is associate with progression to a more advanced phases of the disease and even death. TKIs resistance can be primary resistance in which patients do not respond at all or secondary resistance in which patients develop resistance during the course of the treatment. Kinase domain (KD) mutations in about 50-90% of patients who relapse under imatinib therapy were reported. Based on one study, KD mutations were seen in 75%, 82%, 52%, and 27% of patients with myeloid blastic phase, lymphoid blastic phase, accelerated phase, and chronic phase, respectively. About 50 KD mutations have been recognized that imatinib cannot overcome but most of these mutations can be captured by nilotinib, dasatinib, and bosutinib. Apart from different mutations, a higher level of BCR/ABL1 transcript in

some patients may confer TKIs resistance especially in the advanced phase of the disease. This higher level of BCR/ABLl1 allows the leukemic cells to survive despite TKIs therapy and to have enough time to develop mutations (20, 21).

1.5- CML stem cells

Another reason for the drug resistance and relapse is related to the presence of CML LSCs in different stages of the disease. It seems CML LSCs are not totally dependent on BCRABL1 kinase activity and some BCRABL1 independent mechanisms guarantee their survival.

B-catenin pathway has major a role in self-renewal and long-term capacity of HSCs and CML LSCs. Confirming this, CML LSCs from B-catenin null mice lose their self-renewal capability during serial transplantation (22, 23). Activation of B-catenin in CML LSCs may occur through BCRABL1 activity, TKIs treatment, or the BMM. It has been reported that BCRABL1 stabilizes B-catenin and leads them toward the nucleus (24). Also, TKIs result in the upregulation of tumor necrosis family ligand CD70 by inhibiting miR-29 (25). This results in an increase in CD27 signaling and activation of the WNT/B-catenin pathway. Also, interaction of CML LSCs with stromal cells activates the B-catenin pathway and increases TKIs resistance (26, 27). Imatinib enhances the nuclear factor of activated T-cells activation by non-canonical WNT signaling pathway. Increased NFAT activity in CML LSCs results in TKIs resistance (28).

The hedgehog pathway also regulates the self-renewal of HSCs and CML LSCs. upon binding of Hedgehog ligand to Ptch receptor, it relives its inhibitory effect on SMO and results in activation of GLI transcription factor family (29). Upregulation of SMO in CML LSCs and their persistence after TKIs therapy may suggest that this pathway is BCRABL1 independent (30). There are several inhibitors for this pathway like

cyclopamine or PF-04449913 that suppress CML LSCs development with low side effects on normal HSCs (31, 32).

PI3K signaling pathway has an important role in the proliferation and maintenance of HSCs and CML LSCs (33). It has been reported that BCRABL1 in CML LSCs activates PIK3/AKT signaling pathway (34). In CML LSCs AKT phosphorylates FOXO transcription factor and sequesters it in the cytoplasm and keeps it in inactive mode. TKIs by downregulation of BCRABL1 kinase activity and PI3K/AK pathway reduces FOXO phosphorylation and lead to relocalization of FOXO to the nucleus. FOXO activation leads to upregulation of BCL6 that is essential for the maintenance of CML LSCs. Also, TGF B by inhibiting AKT activity and results in activation of FOXO (35).

Also, BCRABL1 activates JAK/STAT signaling pathway (36). Targeting JAK-2 results in apoptosis of resistant CML stem/progenitor cells to imatinib (37). Meanwhile, a combination of imatinib with interferon gamma reduces STAT5 phosphorylation and enhancement of STAT1 phosphorylation. This might increase CML LSCs survival by the same mechanism as FOXO via upregulation of BCL6 (38). Also enhanced activity of JAK/STAT in CML LSCs compared to healthy counterparts might help to target them selectively. As the combination of nilotinib with ruxolitinib significantly targeted CML LSCs (39). Signaling pathways in CML LSCs are shown in Figure-1.

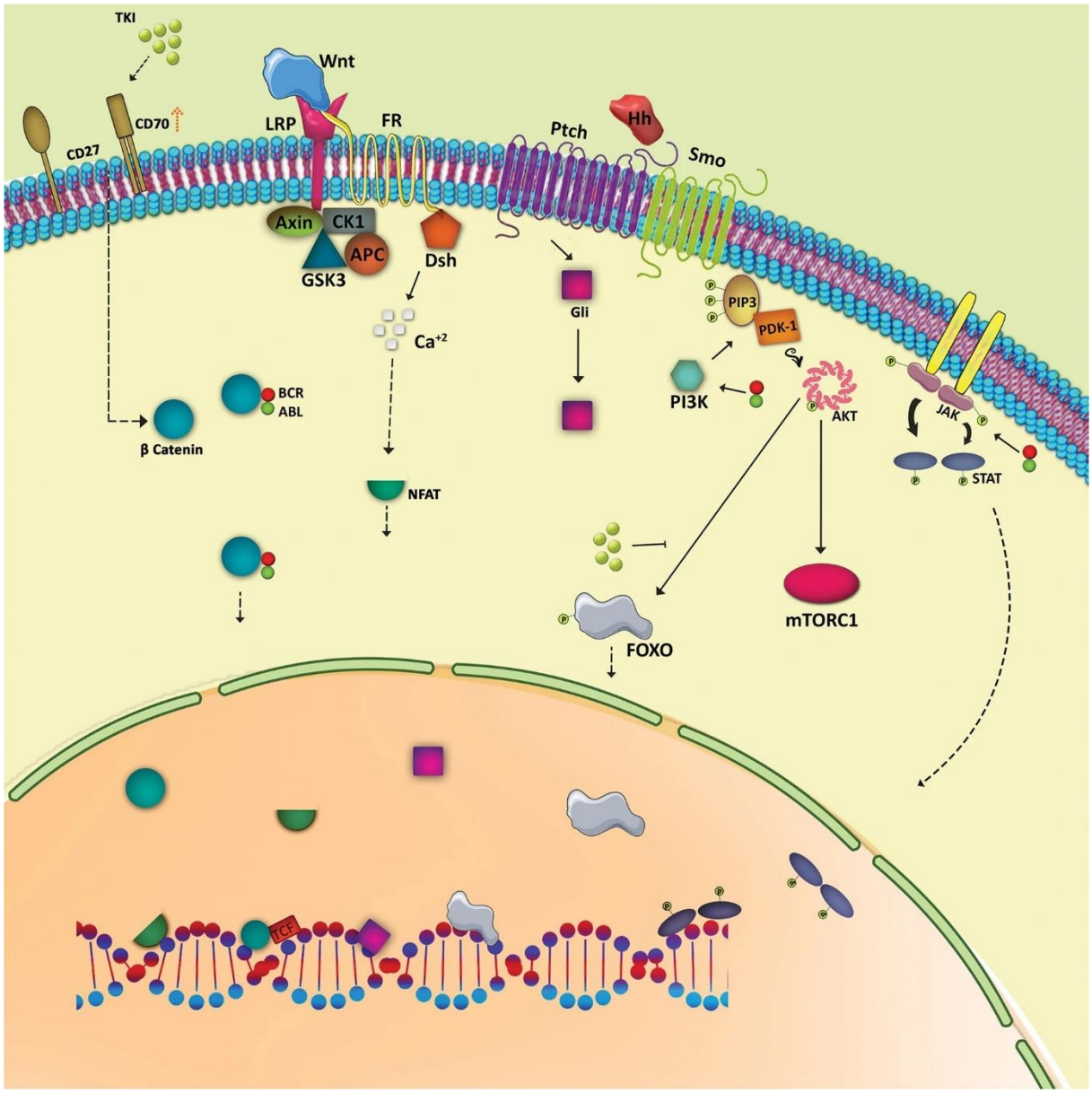

Figure 1. Signaling pathways in CML LSCs.

Also, bone marrow microenvironment (BMM) preserves CML LSCs and provide a decent ambiance for their progression. BMM is composed of many cell types which through physical interactions or secretion of different stimuli regulates the function of HSCs and LSCs (40). A different study reported the negative relation between BCRABL1 and CXCR4 (41). Targeting BCRABL1 by TKIs leads to upregulation of CXCR4. Enhanced activity of CXCR4 in CML LSCs results in their lodgement to the BMM which is concomitant with drug resistance (41, 42). Also, CML LSCs in contrast

with their normal counterpart are not dependent on VLA-4 and VLA-5 for the homing (43, 44). It has been reported that E and L-selectin and related ligands such as CD44 plays an important role in CML LSCs homing (44). Meanwhile, TKIs exposure may lead to adhesion of CML LSCs to stromal cells through N-cadherin that may result in activation of the B-catenin pathway and protection against TKIs (26).

Meanwhile, CML LSCs and the BMM have mutual interactions with each other. For instance, CML LSCs activate the epidermal growth factor pathway in stromal cells by secretion of exosome containing amphiregulin. This leads to enhanced secretion of IL-8 by stromal cells that support CML LSCs survival (45). Also, enhanced BMPR1b level in CML LSCs and binding to BMP2/4 through paracrine and autocrine manner results in TKIs resistance (46, 47). Also, BCRABL1 activity in CML LSCs results in phosphorylation of SPRED1 and following downregulation of miR-126 that has a role in CML LSCs quiescence. Endothelial cells in the BMM by trafficking miR-126 through extracellular vesicle support CML LSCs quiescence(48). Other studies claimed that stromal cells by reducing reactive oxygen species (ROS) in CML LSCs or secretion of FGF2 increase TKI-resistance of CML LSCs (49, 50).

Although the focus of the therapy is on targeting BCR/ABL tyrosine kinase activity, it is worth mentioning that BCR/ABL transcript is also detectable in some healthy people. This might confirm that BCR/ABL should be present in a cell that has the biological potential to cause leukemia. So instead of focusing on BCR/ABL, targeting these biological differences between normal and leukemic cells might boost the number of patients attaining TFR (51). Structural and functional features of the bone marrow microenvironment is shown in Figure 2.

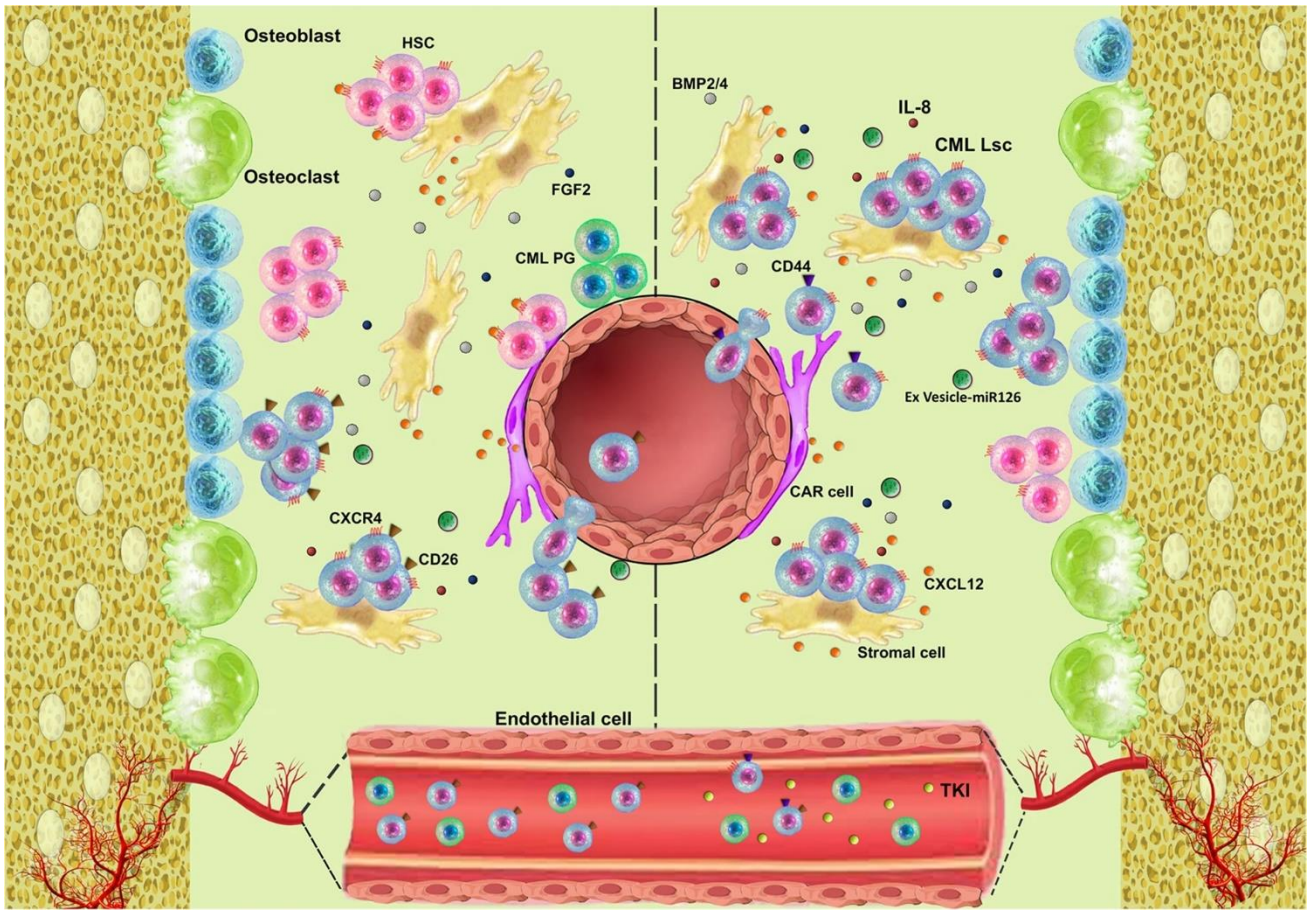

Figure 2. Structural and functional features of the bone marrow microenvironment.

1.6- Dihydroorotate dehydrogenase

Progression and drug resistance of leukemic cells depends on require metabolic rewiring state and increase in energy production. This adjustment mainly occurs through mitochondria as the pivotal metabolic organelle and as a key place for the production of ATP, and management of other cellular processes including apoptosis, differentiation, and also the production of building blocks such as amino acids and nucleotide (52).

Pyrimidine supply in non-proliferating cells is mainly contingent on the salvage pyrimidine pathway which is energetically affordable. However, fast proliferating

leukemic cells need a high level of nucleotides to fulfill their needs. In order to compensate for these high demands nucleotide production via the *de novo* pathway become active in these cells. While the increased activity of the *de novo* pathway provides sufficient nucleotides for leukemia development it may also be used for leukemia targeting. Dihydroorotate dehydrogenase (DHODH) is a vital enzyme in the *de novo* pyrimidine biosynthesis pathway and it is located in the inner membrane of mitochondria. DHODH catalyzes the fourth step of the pyrimidine biosynthesis pathway by oxidation of dihydroorotate to orotate and transfers electrons to ubiquinone as an electron acceptor (53). It has been reported that DHODH inhibition in AML cells is concomitant with unlocking the differentiation block and elimination of residual disease burden. Other studies on different hematological malignancies such as acute lymphoblastic leukemia, myelodysplastic syndrome, and lymphoma revealed that DHODH inhibition could induce apoptosis (53-57). The different responses might be related to the potency of a DHODH inhibitor and it might be context-dependent. The de novo pyrimidine biosynthesis pathway is shown in figure 3.

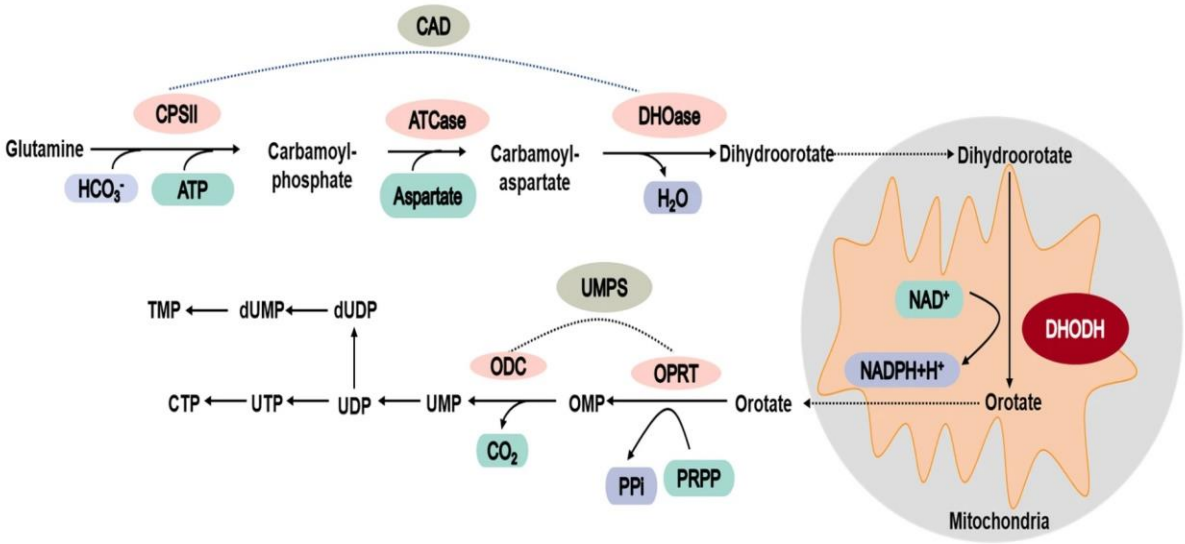

Figure 3. De novo pyrimidine biosynthesis pathway.

1.7- DHODH inhibitors

DHODH inhibitors such as leflunomide and its active metabolite teriflunomide have been used as immunosuppressive agents for the treatment of rheumatoid arthritis and multiple sclerosis, respectively. Brequinar another DHODH inhibitor with higher potency and selectivity compared to leflunomide and teriflunomide has been administered for the treatment of solid tumors. Despite its in vitro effectiveness, it failed to prove its efficacy in clinical trials (53). In 2016, a study by Sykes et al. showed that targeting DHODH by brequinar unblock differentiation arrest in leukemic cells (58). Following this study, other agents with higher potency such as BAY2402234, PTC299, ASLAN003 have been introduced. In contrast with AML, differentiation therapy in CML is not the main goal of treatment, and developing a more potent DHODH inhibitor that can eliminate leukemic cells while preserving its selectivity is of paramount importance.

Previously, a new and potent DHODH inhibitor called Meds433 was developed by our group (56). In the present study, we shed light on the role of DHODH inhibition in CML stem/progenitor cells and how it can be a promising approach in the treatment of CML.

2- Aim of the study

This project was designed to find out the possibility of targeting CML leukemic cells based on their metabolic state. As leukemic cells proliferate more in comparison to healthy cells, a higher nucleotide pool is needed to support their growth. De novo pyrimidine biosynthesis pathway is present and active in healthy cells but their activity is kept at the basal level. So higher activity of this pathway in leukemic cells gives us this opportunity to target leukemic cells and to have minimal impact on healthy cells.

1- **Is DHODH active in CML stem/progenitor cells?**

   To find out if this pathway is active in leukemic cells we treated leukemic cells with different concentrations of DHODH inhibitor. Then we measured apoptosis rate of CML CD34+ primary cells, and CML cell lines following the treatment with Meds433.

2- **Is targeting DHODH suppress CML stem/progenitor cells growth?**

   To check if DHODH inhibition suppresses CML cell growth and causes cell cycle arrest, we performed cell cycle and cell growth analysis. Based on previous reports targeting DHODH in other malignancies caused S/G2M arrest and led to suppression of cell growth.

3- **Is Meds433 is a selective agent for targeting DHODH?**

   To find out if our agent works selectively, we used exogenous uridine and we measured cell viability in treated cells. This experiment also confirms if the de novo pyrimidine biosynthesis pathway is active in CML cells.

4- **Through which mechanism Medds433 might induce cell death?**

To find out which are genes up-regulated or down-regulated following DHODH inhibition, we performed RNA seq. Also, metabolic analysis revealed the metabolic changes following DHODH inhibition in CML cells.

5- Does Meds433 effective in vivo?

As the effect of some agents in vitro might be different than in vivo, we sued a xenograft mice model. After treating with different concentrations of Meds433 we measured, tumor growth, tumor weight, and tumor burden.

3- Materials and methods

3.1- Reagents

Meds433 and Brequinar were synthesized as described in Sainas 2018. Reagents were dissolved in DMSO and diluted in culture media before use. The final DMSO concentration did not exceed 0.1%. Imatinib, uridine and 2′,7′-Dichlorofluorescin diacetate (DCFDA) were purchased from Merck (Milan, Italy). Cytokines were purchases from Miltenyi Biotec, Italy.

3.2- CML samples collection

For this study, 70 Bone Marrow (BM) and Peripheral Blood (PB) samples of newly diagnosed and 4 TKI-resistant CML patients were collected as part of the Italian national study GIMEMA CML1415—Sustrenim, approved by the Ethical Committee of the Coordinating Centers on 11 May 2016.

3.3- Cell culture

For *ex vivo* study, Mononuclear cells (MNCs) were isolated from both BM and PB using Ficoll-Hypaque (Sigma Aldrich, Milan, Italy). Then, CML CD34+ cells were positively isolated by immunomagnetic separation (MACS, Miltenyi Biotec, Italy) and cultured in serum-free stemMACS media (Miltenyi Biotec, Italy) with recombinant human Flt3L (100ng/mL), SCF (100ng/mL), IL3 (20ng/mL), and TPO (20ng/mL). All of the *ex vivo* experiments were performed on CML CD34+ population as CML stem/progenitor cells.

The Bcr-Abl-positive cell lines K562, KU-812, JURL-MK1, and CMLT-1 were maintained in RPMI 1640 (Gibco, Thermo Fisher Scientific) supplemented with 10% heat-inactivated fetal bovine serum (FBS, Gibco, Thermo Fisher Scientific). The

Imatinib-resistant AR230R cell line was cultured in the presence of 1 μM Imatinib. The human mesenchymal stromal cells HS-5 was cultured in DMEM (Microtech, Naples, Italy) supplemented with 10% FBS. Media were supplemented with 1% penicillin/streptomycin (Gibco, Thermo Fisher Scientific). Cell lines were maintained in culture for no longer than 5-6 weeks and were routinely tested for mycoplasma contamination.

For treatment, CML CD34+ and CML cell lines were seeded 10,000 cells/well and incubated at 37°C with Meds433 or DMSO, as the vehicle, for 72 hours at indicated concentrations.

3.4- Apoptotic assay

After treatment of CML CD34+ cells with Med433 from 1nM to 10μM and CML cell lines with Med433 and BQ from 1nM to 10μM, the percentages of viable cells were determined by flow cytometry analyses using Annexin V-FITC Kit (Miltenyi Biotec, Italy), according to the manufacturer's instructions. After the PI addition, samples were acquired on FACSVerse and analysed by Kaluza software version 2.1 (Beckman Coulter Fullerton, CA). To study the selectivity of Meds433, exogenous uridine 100μM was added to the culture media of four CML cell lines treated with Meds433 10μM, and Annexin V was assessed.

3.5- Cell cycle analysis

Cell cycle was measured by Vybrant DyeCycle orange stain (Thermo Fisher) according to the manufacturer's instructions. CML CD34+ and CML cell lines were treated with Meds433 from 1nM to 1μM for 72 hours. Cells were collected, washed with Phosphate buffered saline (PBS), and incubated at 37 °C for 30 min with the dye. Samples were acquired by FACSVerse and data were analyzed with Kaluza software.

3.6- Cell growth assay

The cell growth rate in four CML lines treated with Meds433 was measured with Cell Counting Kit-8 (CCK-8, Microtech, Naples, Italy) according to the manufacturer's instructions. Briefly, CML cell lines were cultured with Med433 from 1 nM to 10µM and after three days, 10 µL of CCK-8 solution was added into each well and incubated for 2 hours. Optical density values were recorded using a plate reader at 450 nm, using a Promega Microplate Reader (Glomax).

3.7- Cell proliferation

The proliferation index of CML CD34+ cells was evaluated by flow cytometry. Briefly, cells were incubated with 1µM carboxyfluoresceindiacetatesuccinimidyl ester **dye** (CFSE, Vybrant CFDA SE cell tracer kit; Molecular Probes, Invitrogen Carlsbad, CA) for 30 min at 37°C. Then they were washed with PBS and incubated in complete media for 30 minutes at 37°. After a wash, labeled CML CD34+ were cultured with or without Meds433 (range 1nM-1µM) for 3 consecutive days. At the end of cultures, cells were collected and the proliferation index was quantified according to the CFSE signal intensity using FCS Express software. Proliferation Index is considered as the total number of cell divisions divided by the number of cells that went into division.

3.8- 3D co-culture

Demineralized bone matrix (DBM, Orthoss Block Geistlich Biomaterial Italia) was coated with collagen type I (100 ug/mL) overnight at 4°C. The coated scaffolds were washed with PBS and centrifuged at 900g for 5 min to unblock the surface pores. $1x10^5$ HS-5 cells were seeded and cultured in DMEM 10% FBS for 24 hours. After a wash with PBS, $1x10^5$ CMLT1 cells labeled CFSE were added to the scaffold in IMDM with 10% FBS. After 24 hours, the scaffolds were washed with PBS to remove

unattached cells. Then the scaffolds were treated with Meds433 100nM for 3 days and the mean fluorescent intensity of CMLT1 labeled CFSE and morphology by the surface electron microscopy was measured.

3.9- RNA sequencing

Gene expression profiling and GSEA Gene expression profiling was performed on CML $CD34^{+}$ treated with Meds433 100nM for three days. Total RNA was isolated using TRIzol reagent (Invitrogen), according to the manufacturer's protocol. Quantity and quality of the starting RNA were checked by Qubit and Bioanalyzer (Agilent). Libraries were prepared using the TruSeq Stranded mRNA Sample Prep Kit (Illumina) following the manufacturer's instructions. Libraries were sequenced on Illumina NextSeq 500 System (single-end 75 bp reads). Sequencing reads were aligned to human reference genome (version GRCh38.p13) using STAR v2.7.7a0 (59) (with parameters –outFilterMismatchNmax 999 --outFilterMismatchNoverLmax 0.04) and providing a list of known splice sites extracted from GENCODE comprehensive annotation (version 32). Gene expression levels were quantified with featureCounts v1.6.3 (60) (options: -t exon -g gene_name) using GENCODE gene annotation (version 32 basic). Multi-mapped reads were excluded from quantification. Gene expression counts were next analysed using the edgeR package (61). Normalization factors were calculated using the trimmed-mean of M-values (TMM) method (implemented in the calcNormFactors function) and RPKM were obtained using normalized library sizes and gene lengths. After filtering lowly expressed genes (below 1 CPM in 6 or more samples), differential expression analysis was carried out by fitting a quasi-likelihood negative binomial generalized log-linear model using patient's identity as a blocking factor and performing QLF test comparing treated and untreated

samples. Genes were considered as significantly differentially expressed (DEGs) when having |logFC| >0.5 and FDR < 0.05.

RPKM values were scaled as Z-scores across samples before computing distances.

Gene Set Enrichment Analysis was performed using GSEA (v 3.0) in pre-rank mode using logFC obtained from the edger model as ranking score. Gene sets in Molecular Signature Database were considered (v7.0), excluding sets bigger than 2500 and smaller than 5 genes.

3.10- RNA isolation and qRT-PCR for mRNA detection

Total RNA was isolated from CML CD34+ using TRIzol® Reagent (Invitrogen Life Technologies). For mRNA detection, 250 ng of DNAse-treated RNA (RQ1, Promega) was retrotranscribed with High-Capacity cDNA Reverse Transcription Kit (Applied Biosystems). qRT-PCRs for mRNA detection were performed with the SYBR® Green PCR Master Mix on cDNAs according to the manufacturer's instructions. qRT-PCRs were carried out using gene specific primers and a 7900HT Fast Real Time PCR System (Applied Biosystems). Quantitative normalization was performed on the expression of β-actin mRNA. The relative expression levels between samples were calculated using the comparative delta CT (threshold cycle number) method (2-ΔΔCT) with a control sample or the median expression of the analyzed genes as reference point. The following Quantitect primer assays (Qiagen) were used: Hs_PLKR_1 QT00016156, Hs_DDIT3_1 QT00082278, Hs_GPT_1 QT01001595, Hs_PLK2_1 QT00049406, Hs_CDKN1A QT00062090, HsAHSP_1 QT00215992, Hs_ACTB_1 QT000945431.

3.11- CFU assay

Primary CML CD34+ were cultured for three days with Meds433 100nM or control and then 500 cells/dish were suspended in IMDM supplemented with 2% FBS. Cells were plated in methylcellulose-containing medium (StemCell Technologies) in 35-mm dishes based on the manufacturer instruction and colonies were scored and counted after 15 days.

3.12- Differentiation markers

CML CD34+ cells were treated with Meds433 100nM for 72h and stained with anti-human CD11c-APC (Miltenyi Biotec), CD318-FITC (Miltenyi Biotec), OSCAR-APC (Miltenyi Biotec), CD1c-FITC (Thermo Fisher), CD61-FITC (Thermo Fisher), and CD41-FITC (Thermo Fisher) at room temperature for 20 min. Data collection was done on FACSVerse and data were processed with Kaluza software version 2.1.

3.13- Measurement of ROS

The cellular ROS production of CML CD34+ cells treated with Meds433 100nM was detected by flow cytometry staining with 15 μM DCFDA for 20 min at 37°C. Then, cells were incubated with pre-warmed media for additional 5 minutes at 37°C. After a wash, fluorescence was measured by FACSVerse using Kaluza software.

3.14- Measurement of Mitochondrial Membrane Potential

The mitochondria membrane potential of CML CD34+ cells was measured following the treatment with Meds433 100nM. After staining with tetrametylrodamine methyl ester (TMRM; Molecular Probes, Eugene, Oregon, USA), according to the manufacturer's instructions cells were washed with PBS, and incubated at 37°C with

20nM TMRM for 30 minutes. Cells were washed and analyzed by FACSVerse using Kaluza software.

3.15- Mitochondria circularity and elongation

Following the CML $CD34^+$ culture without or with Meds433100nM, the image acquisition was performed with a Leica TCS SP5 confocal system (Leica Microsystems) equipped with a HCX PL APO 63×/1.4 NA oil-immersion objective. Images were acquired on the three coordinates of the space (XYZ planes) with a resolution of 70 nm x 70 nm x 300 nm for at 8-12 cells/condition.

To quantify mitochondria circularity and elongation, an ImageJ (Rasband, W.S., U.S. National Institutes of Health, Bethesda, MA) macro was created. Briefly, images were pre-processed with background subtraction and Gaussian blur and segmented using intensity thresholding; binary images were post-processed to improve mitochondrial detection, finally, the circularity was measured:

circularity = 4pi(area/perimeter^2)

A circularity value of 1.0 indicates a perfect circle. As the value approaches 0.0, it indicates an increasingly elongated shape. Inverse circularity was used as a measure of mitochondrial elongation.

3.16- Senescence assay

Following the treatment with Meds433 (100nM), CML CD34+ cells were stained using cellular Senescence detection kit-SPiDER-βGal (Dojindo Molecular technologies) according to the manufacturer's instructions. Briefly, cells were incubated with bafilomycin A1 at 37 °C for 1 h. Cells were further incubated for 30 minutes at 37 °C with then SPiDER-βGal solution. After a wash, cells were acquired using FACSC Verse and analyzed with Kaluza software.

3.17- Metabolic profile analysis

A targeted metabolic profile was measured by the MxP® Quant 500 kit (Biocrates Life Sciences AG, Innsbruck, Austria). This kit measures 630 metabolites from 26 biochemical classes. The metabolites were extracted from CML CD34+ cells treated with Meds433 100nM for three days. The experimental metabolomics measurement techniques are described in detail by patents EP1897014B1 and EP1875401B1. Briefly, a 96-well based sample preparation device was used to quantitatively analyse the metabolite profile in the CML CD34+ samples. This device consists of inserts that have been impregnated with internal standards, and a predefined sample amount was added to the inserts. Next, a phenyl isothiocyanate (PITC) solution was added to derivatize some of the analytes (e.g. amino acids), and after derivatization was completed, the target analytes were extracted with an organic solvent, followed by a dilution step. The obtained extracts were then analysed by FIA-MS/MS and LC-MS/MS methods using multiple reaction monitoring (MRM) to detect the analytes. Concentrations were calculated using appropriate mass spectrometry software (Sciex Analyst) and normalized as picomoles per million cells. Further data analysis has been performed using MetaboAnalyst (versio 5.0). Out of 630 features, 435 have a constant or single value across all 10 analyzed samples and were removed, 54 were removed because under level of detection in more than 60% of samples. Missing variables were replaced by LoDs (1/5 of the min positive value for each variable). Data were normalized using a Probabilistic Quotient Normalization using control patients as reference group (62), log10 transformed and Pareto scaled.

The heatmap in figure 7A, the metabolites with FDR<0.1 (paired t-test) are reported, the represented values are log fold change concentrations between treated and

relative control samples. Among many significantly increased Phosphatidylcholine detected, only one is reported as representative of the entire metabolite class.

3.18- CML xenograft mouse model

KU-812 cells (1×107cells in PBS mixed 50:50 with Matrigel™ (BD, Bioscience) were implanted subcutaneously into the left flank of 13-week old NOD/SCID/γ chain-/- (NSG) immunocompromised mice. Mice were randomized into control or Meds433 treated groups when the volume of masses reached approximately 0,2 cm^3 and was palpable. Mice were treated intraperitoneal for 21 consecutive days with vehicle (7% DMSO and 93% corn oil from Sigma Aldrich), Meds433 10mg/kg, and 20mg/kg. The tumor volume was measured once a week with a caliper and calculated with V= 1/2 × (length × width2). Mice were treated following the European guidelines and with the approval of the Italian Ministry of Health (Authorization n. 42/2020-PR). Mice were euthanized when the dimension of tumors in the control group exceeded the size of 1.5cm^3 at the end of the experiment. Then, PB, BM, and spleen were collected to evaluate tumor burden by flow cytometry, using hCD45+ (Invitrogen, Life Technologies). Also, hematoxyline and eosin staining of the tumor xenografts was performed.

3.19- Plasma level of Meds433 and its metabolite in treated mice

Plasma samples of treated mice were analyzed using a high-resolution mass spectrometer (HRMS) (Q-Exactive Orbitrap, Thermo Scientific) coupled to an HPLC instrument (1200 system Agilent). Chromatographic separation was carried out on an Ascentis C18 column (150 × 2.1 mm; 2.7-µm particle size, Sigma-Aldrich, St. Louis, MO) maintained at 35 °C. The elution mixture was composed of solvent A (HCOOH

0.1% in water) and solvent B (acetonitrile). The elution gradient was from 10 to 99% of solvent B in 12 minutes; hold at 99% for 4 minutes and re-equilibration for 4 min at 10% of solvent B. The volume of injection and flow rate were 4µL and 160µL/min, respectively. The mass spectrometric analyses were performed in positive ion mode using a HESI II source and with the following conditions: heated capillary temperature 320 °C, spray voltage 3 kV (positive ions), auxiliary gas temperature 200 °C, flow rate 6, sheath gas flow rate 32, sweep gas flow rate 2 (arbitrary units). Accurate mass measurements were obtained with full scan mass acquisition (resolving power R = 35,000; mass range: m/z = 200-700 Da). Data were acquired and elaborated using Xcalibur Browser (Thermo Fisher Scientific, Waltham, MA, USA). For sample preparation, fifty microliters of plasma were diluted with 200µL of ethanol containing 5 ng of M489, used as internal standard. Samples were vortexed and centrifuged at 13 200 rpm for 15 min; 4µL aliquots of the supernatants were injected directly into the HPLC-HRMS system.

4- Results

4.1- DHODH inhibition induces apoptosis in CML

Previously, we reported that Meds433 significantly induces apoptosis and differentiation in AML cells. To study the effect of DHODH inhibition in the induction of apoptosis in CML, an apoptosis assay was performed. Treatment with various concentrations of Meds433 (1nM to 10µM) displayed a significant apoptotic effect in different CML cell lines and sorted CML CD34+ cells (Fig. 1A). The starting concentration that remarkably reduced cell viability in CML stem/progenitor cells was 100nM. To expand these results and to study the effect of Meds433 on resistant TKIs cells, resistant CML CD34+ and AR-230R (a cell line resistant to imatinib) were treated with Meds433. As shown in Fig. 1B, DHODH inhibition induced apoptosis in resistant cells starting from 100nM, and this effect increased in a dose-dependent manner.

To confirm the selectivity of our agent in targeting the pyrimidine biosynthesis pathway, exogenous uridine was employed. As is shown in Fig. 1C, the addition of uridine to the culture media abolished the apoptotic effect of Meds433 10µM in four different CML cell lines. This result proves the selectivity of this inhibitor in targeting the DHODH enzyme.

We also measured the apoptotic effect of BQ in CML-T1 and K562 cells. Based on the obtained results (Fig. 1D), BQ did not show any effect at low concentrations and its activity was seen at high concentrations of 1µM and 10µM. This result shows the potency of our agent as a new generation of DHODH inhibitor in comparison to BQ. EC50 of Meds433 and BQ in CML cells is shown in Fig. 1E.

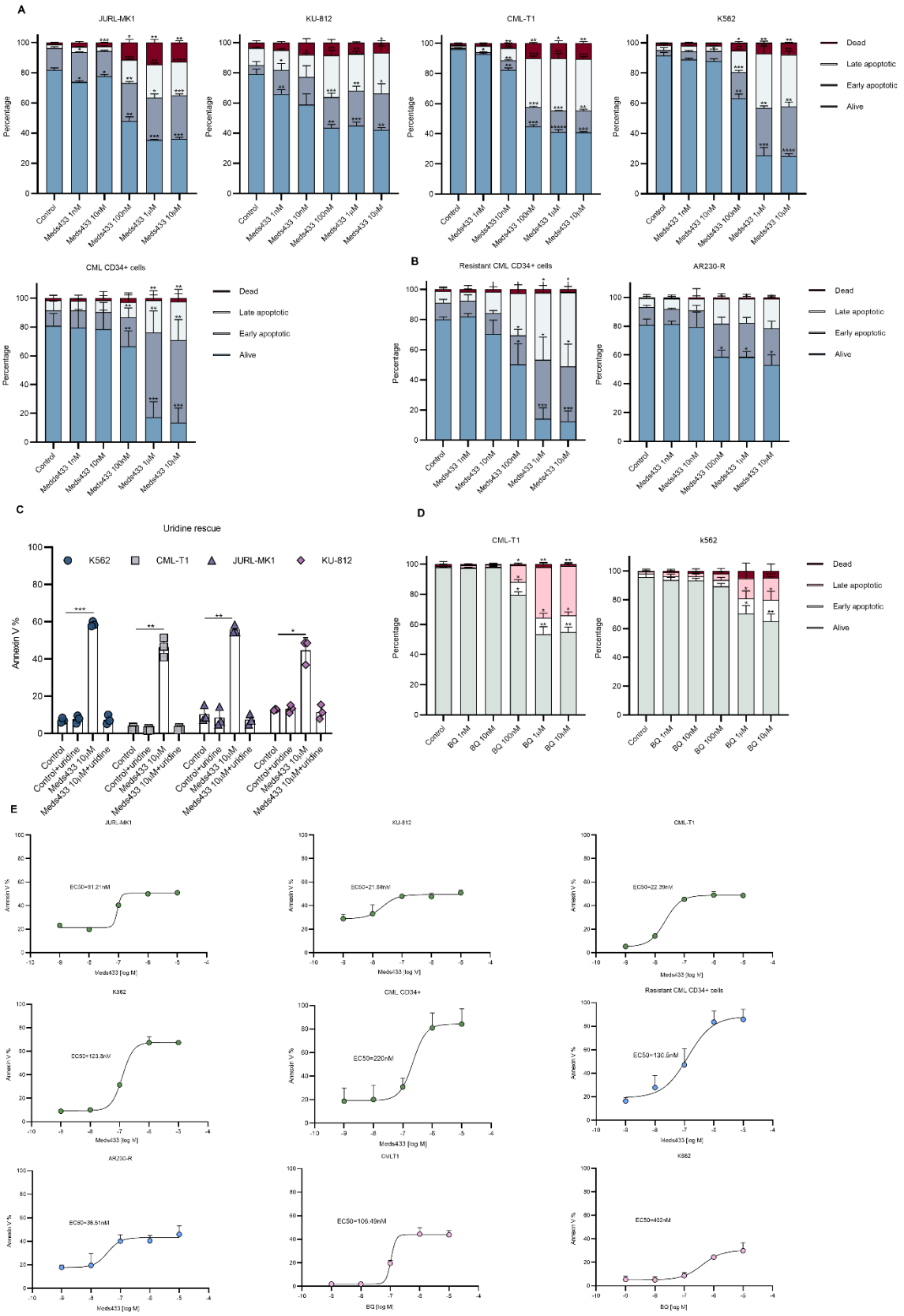

Figure 1. DHODH inhibition induces apoptosis in CML. (A) demonstrates apoptosis in CML cell lines and newly diagnosed CML CD34+ (n:6) after the treatment with various concentrations of Meds433.

(B) represents the effect of Meds433 on resistant CML CD34+ cells (n:4) and AR-230R a cell line resistant to imatinib. Addition of uridine to the culture media rescued apoptotic phenotype in CML cell lines treated with 10μM of DHODH inhibitor (C). Also, apoptotic effect of BQ was measured in CML-T1 and K562 cells (D). EC50 of Meds433 and BQ in CML cells is displayed in (E). * p<0.05, ** p<0.01, *** p<0.001, **** p<0.0001, **** p<0.00001.

4.2- DHODH inhibition induces cell cycle arrest and suppresses CML cell growth

We measured the cell growth rate and the proliferation index in CML cell lines and CML primary cells. As is shown in Fig. 2A, treatment of CML cell lines with Meds433 (1nM to 10μM) hampered cell growth rate. To confirm these results in CML stem/progenitor cells, CML CD34+ were labelled with CFSE, and proliferation index was measured by flow cytometry. As is shown in Fig. 2B, DHODH inhibition could suppress the proliferation of CML CD34+ cells.

This cell growth arrest implied that we have a cell cycle arrest in CML cells following DHODH inhibition. Following the treatment of CML cells with different concentrations of Meds433, cell cycle was analyzed. As it is displayed in Fig. 2C, treatment of CML CD34+ cells with different concentrations of Meds433 induced cell cycle arrest in the G2/M phase. This arrest was started at the concentration of 100nM while a reduction in G0/G1 phase was seen at 10nM. The pattern of the G2/M arrest was similar in KU-812, CML-T1, JURL-MK1, and K562 but the concentrations that caused this arrest were different. In primary cells and CML cell lines the degree of DHODH inhibition able to induce cell cycle arrest started at low concentrations (1nM or 10nM) and reached its apex at 100nM.

Also, many reports claimed that stromal cells and bone marrow microenvironment might compromise the impact of different drugs on leukemic cells. To address this

point, we mimicked the bone marrow microenvironment using a 3D-coculture platform. Our results proved that treatment of CML-T1 with Meds433 100nM reduced their proliferation rate in 3D-coculture condition and impeded their expansion (Fig. 2D). The surface electron microscopy (SEM) images of this 3D-coculture experiment are shown in Fig. 2E. SEM data revealed that CML-T1 colonies were eliminated after DHODH inhibition.

After performing CFU assay our results showed that the total number of colonies significantly decreased in CML CD34+ treated with Meds433 100nM (Fig. 2F, left panel). However, we found that this decrease was related to CFU-E and BFU-E potential (Fig. 2F, right panel). This might be related to the negative effect of DHODH inhibition on genes involved in erythropoiesis. Also, we had an increase in CFU-GM (Fig. 2F, right panel), that proves the tendency of a cell with stem cell potential toward myelomonocytic lineage under stress conditions.

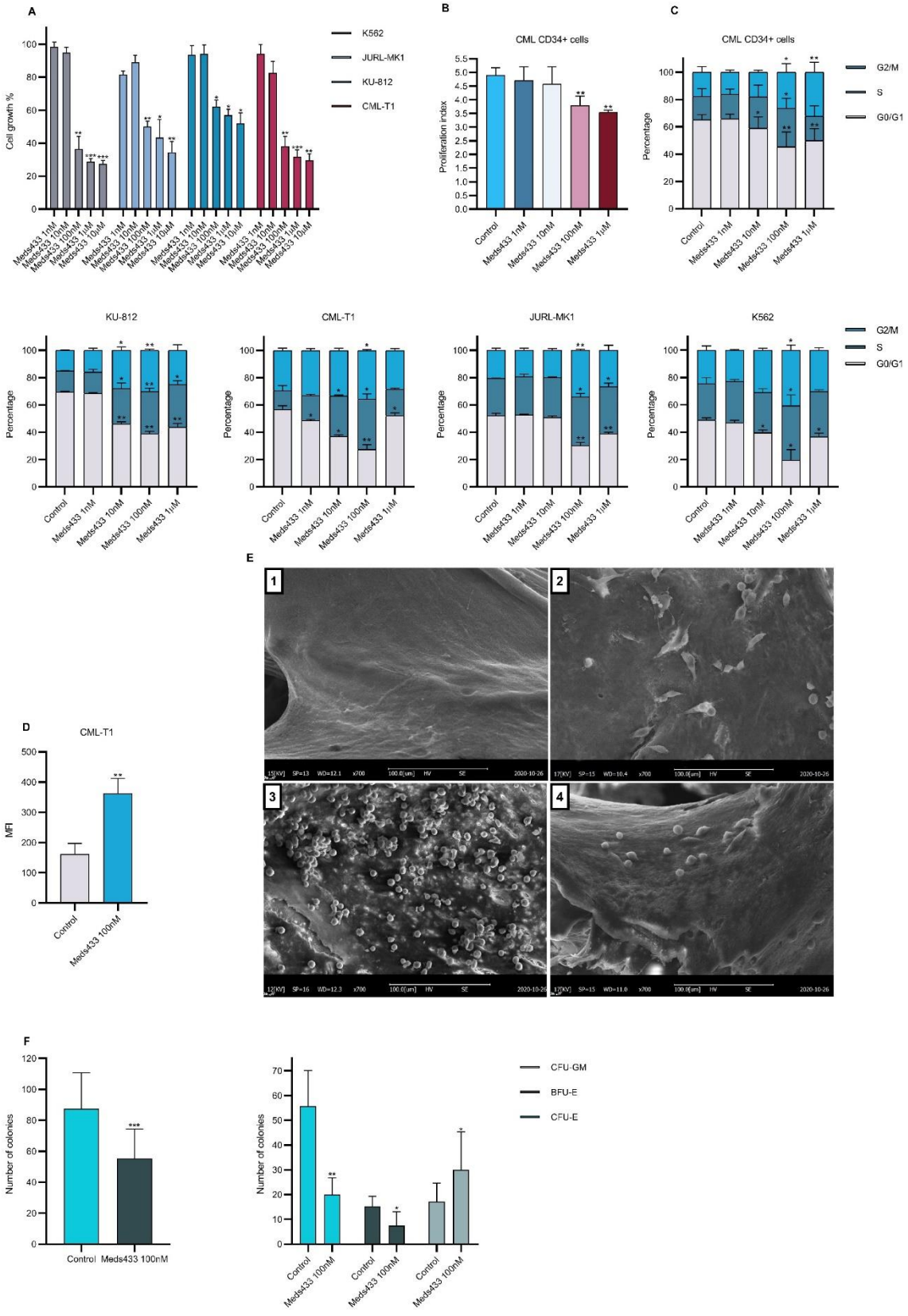

Figure 2. Effect of DHODH inhibition on cell cycle and cell growth rate. Cell growth assay by CCK8 assay in cell lines and proliferation index in CML CD34+ (n:3) by flow cytometry analysis are displayed

in (A) and (B), respectively. Cell cycle analysis in CML CD34+ (n:6) and four different CML cell lines are shown in (C). Mean fluorescent intensity (MFI) of CFSE-labelled CML-T1 treated with Meds433 100nM in a 3D co-culture platform is shown in (D). Electron microscopy images of the 3D co-culture platform are displayed in (E). Demineralized bone matrix (DBM) treated with collagen type 1 (E-1). Mesenchymal stromal cells (MSCs) in DBM scaffold (E-2). Addition of labelled CML-T1 with CFSE to the MSCs in the scaffold (E-3). 3D-co-culture condition treated with Meds433 100nM (E-4). Number of colonies after the treatment of CML CD34+ (n:5) with Meds433 is shown in (F). * $p<0.05$, ** $p<0.01$. *** $p<0.001$.

4.3- Meds433 significantly changes transcriptome in CML CD34+

To demonstrate the effect of DHODH inhibition on transcriptome profiling of CML CD34+, RNA-seq was performed. By considering 0.5-log fold expression level and FDR<0.05 as the cutoff for both up and down-regulated genes, we observed that the number of upregulated genes (1598 genes) was higher compared to the down-regulated ones (876 genes) (Fig. 3A). Considering the top 100 differentially expressed genes (in terms of P-value), upregulated genes were mostly related to apoptosis, movement, and differentiation toward myeloid lineage (in line with CFU assay). Genes related to erythropoiesis (in line with CFU assay), proliferation, and metabolism were downregulated after the treatment (Fig. 3B). Then gene set enrichment analysis (GSEA) was performed to reveal gene sets that were enriched or depleted after the treatment with Meds433 (Fig. 3C). The significantly enriched hallmark gene sets were mainly related to inflammation (such as interferon-γ, interferon-α, TNF-α, TGF-β), survival pathways (such as apoptosis, P53 pathway), and immune response (such as IL2-STAT5, complement). On the other hand, gene sets germane to cell cycle and proliferation (such as MYC targets, E2F targets, G2/M checkpoints), metabolism (such as heme metabolism, oxidative phosphorylation, fatty acid metabolism, glycolysis)

were depleted. Some GSEA enrichment plots are displayed in Fig. 3D. The validation by qRT-PCR confirmed some differentially expressed genes (Supplemental Figure 1A). Western blot analysis confirmed alterations in apoptosis and known genes previously reported (Supplemental Figure 1B). These results suggest the induction of metabolic stress in leukemic cells after treatment with Meds433.

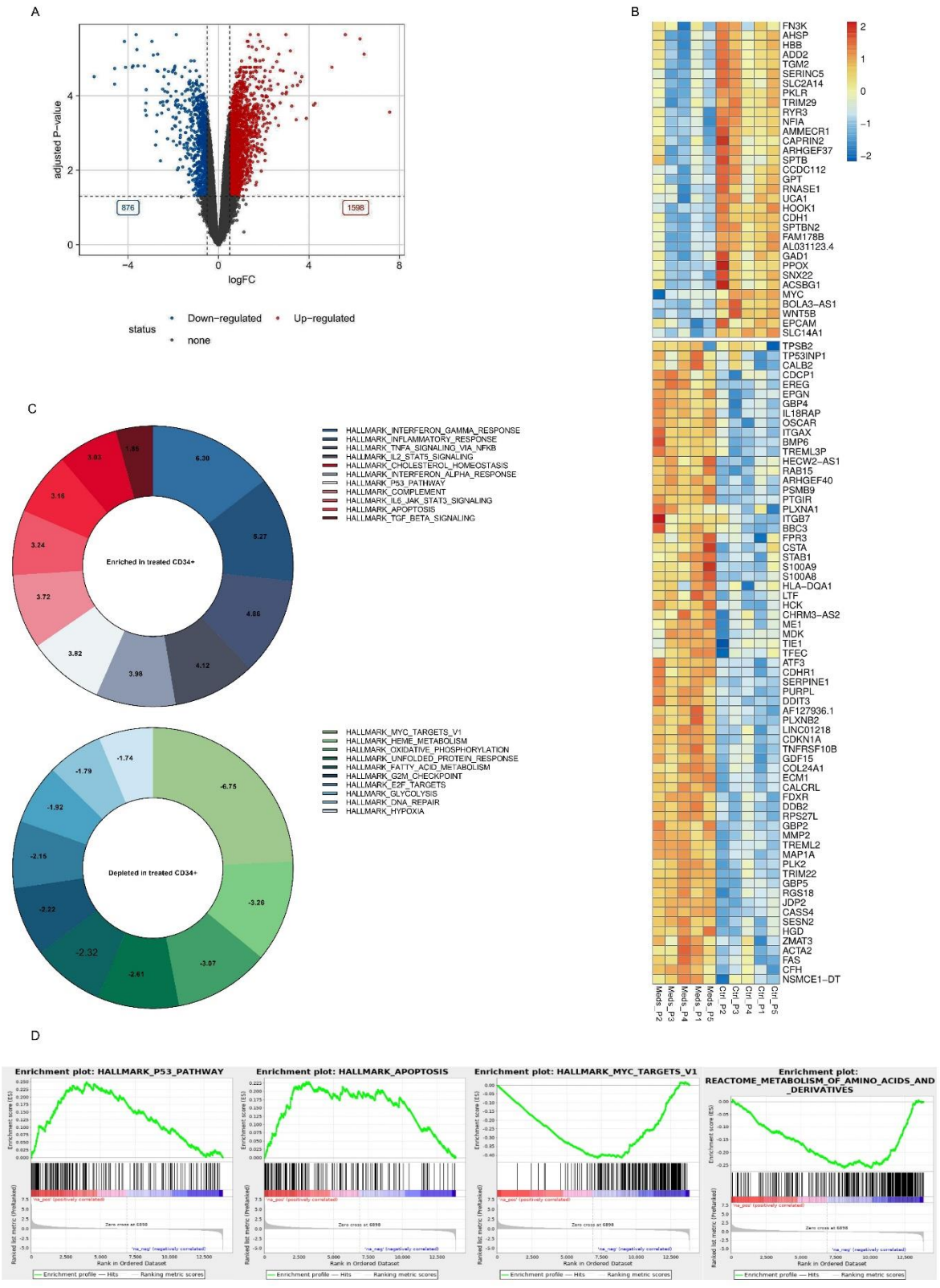

Figure 3. RNA-seq analysis following DHODH Inhibition in CML. (A) the Volcano plot demonstrates the number of up and down-regulated genes in CML CD34+ (n:5) after treatment with Meds433 100nM. Top 100 differentially expressed genes based on adjusted p-value are depicted in the heatmap (B),

enriched and depleted hallmark gene sets are shown in (C). The number in the plots demonstrates a normalized enrichment score (NES). Some pathways that were enriched or depleted are shown in (D).

4.4- DHODH inhibition increases maturation markers and disrupts the normal function of mitochondria

As described previously, DHODH inhibitors induce differentiation of AML cells toward myeloid lineage. To check if we have any differentiation effect in CML and based on the result of RNA seq, lineage-specific cell surface markers were measured. After the treatment of CML CD34+ with Meds433 100nM, we found a significant Increase in CD11c, CD1c, OSCAR (marker of dendritic cell and monocyte lineage), CD318 (a marker of cell migration) and CD61, CD41 (megakaryocytic markers) (Fig. 4A).

Also, DHODH inhibition in CML CD34+ increased ROS production and reduced mitochondria cell membrane potential (Fig. 4B). This phenomenon is known to eventually result in mitochondria damage and subsequent apoptosis.

Inflammation profile, cell cycle arrest, cell growth arrest, and ROS production implied that treated CML CD34+ cells might undergo senescence and lose their self-renewal capability. To prove this, we measured β-galactosidase in CML CD34+ treated with Meds433 100nM and a significant increase in β-galactosidase level was recorded (Fig. 4C).

To demonstrate the role of DHODH inhibition on mitochondria morphology we analyzed structural features of mitochondria by confocal microscopy. Our results showed that DHODH inhibition is concomitant with reduction of elongation and enhancement of circularity in mitochondria (Fig. 4D). Confocal images of one CML CD34+ treated with Meds433 100nM are displayed in Fig. 4E.

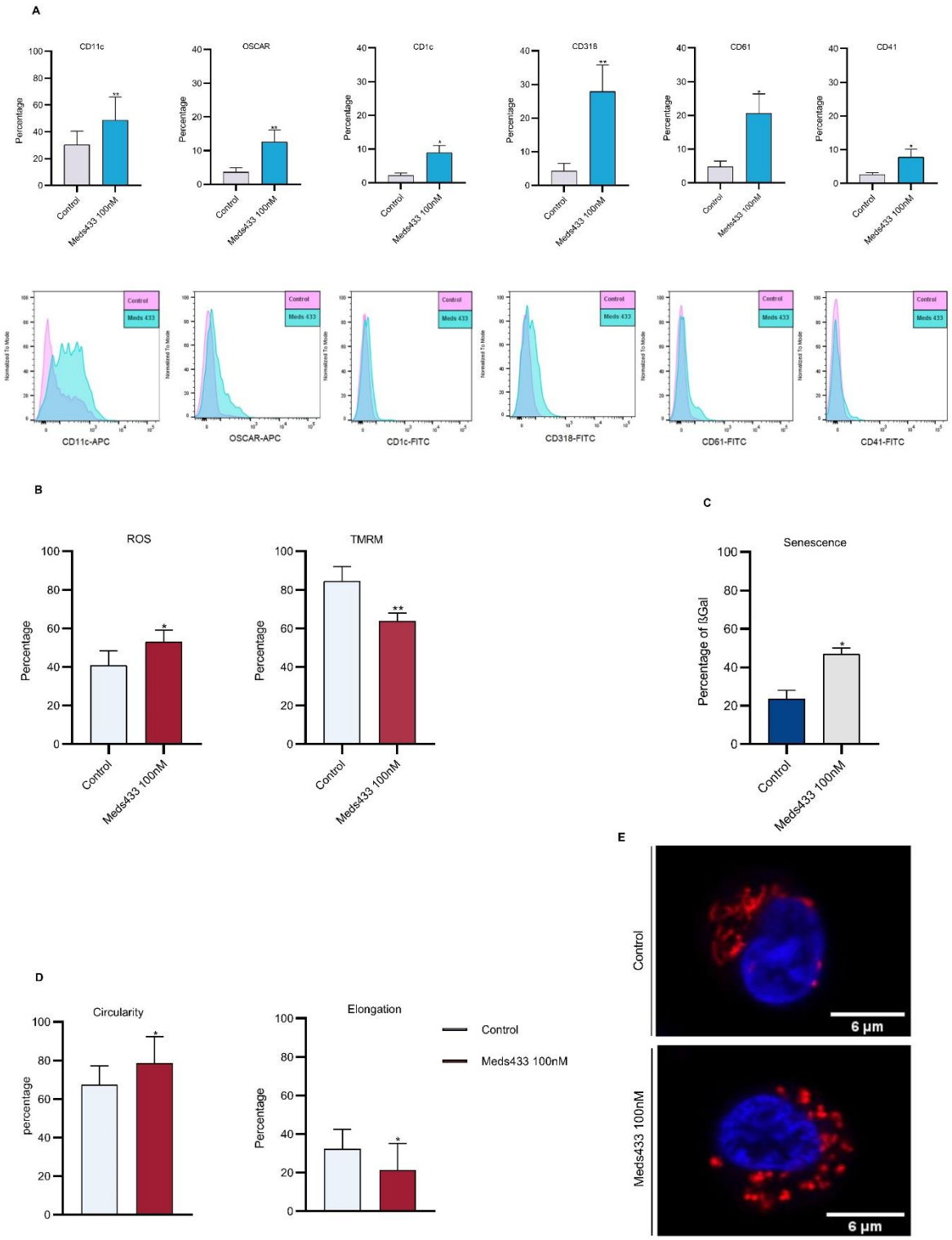

Figure 4. DHODH inhibition induces differentiation and disrupts mitochondria function in CML. Expression of lineage-specific CD markers after the treatment of CML CD34+ (n:21) with Meds433 is displayed in (A). Targeting DHODH led to an increase in ROS production and reduction of

mitochondria cell membrane potential in CML CD34+ (n:5) (B). β-galactosidase level in CML CD34+ (n:3) after DHODH inhibition is shown in (C). Percentage of mitochondria with circularity>0.8 and elongation>1.25 in CML CD34+ (n:4) is shown in (D). Confocal images of one CML CD34+ sample treated with Meds433 100nM are shown in (E), where the nucleus was labeled with Hoechst dye (blue) and mitochondria were labeled with MitoTracker (red). * $p<0.05$, ** $p<0.01$.

4.5- Targeting DHODH alters metabolic profile in CML stem/progenitor cells

To demonstrate the effect of DHODH inhibition on the metabolic state of CML stem/progenitor cells, 630 metabolites were quantified. Permutation test on OPLS-DA analysis shows that samples can be correctly classified as treated or controls according to metabolites concentrations (Q2 Pvalue = 0.025, R2Y Pvalue = 0.053 over 1000 permutations). Our results showed that amino acids decreased after the treatment with Meds433 100nM in CML CD34+ (Fig. 5A). Among these amino acids, glutamine is of high importance as it is a key component of the pyrimidine biosynthesis pathway. Also, the reduction of amino acids might mediate the different cellular responses caused by DHODH inhibition. For instance, redox balance in cells is managed by glutamate, glycine, and cysteine that decreased in CML CD34+ after treatment. Also decrease of biogenic amines like putrescine and spermidine that promote tumor growth highlights the key role of DHODH in leukemic cell development. Meanwhile, Meds433 reduced lactate production in CML cells as an important oncometabolite in cancer progression. On the other hand, an increase in phosphatidylcholines, ceramides, and sphingomyelins that have a role in apoptosis differentiation and senescence in treated cells is in line with previous findings (Fig. 5A). Concentrations of some metabolites in treated and untreated CML CD34+ are shown in Fig. 5B.

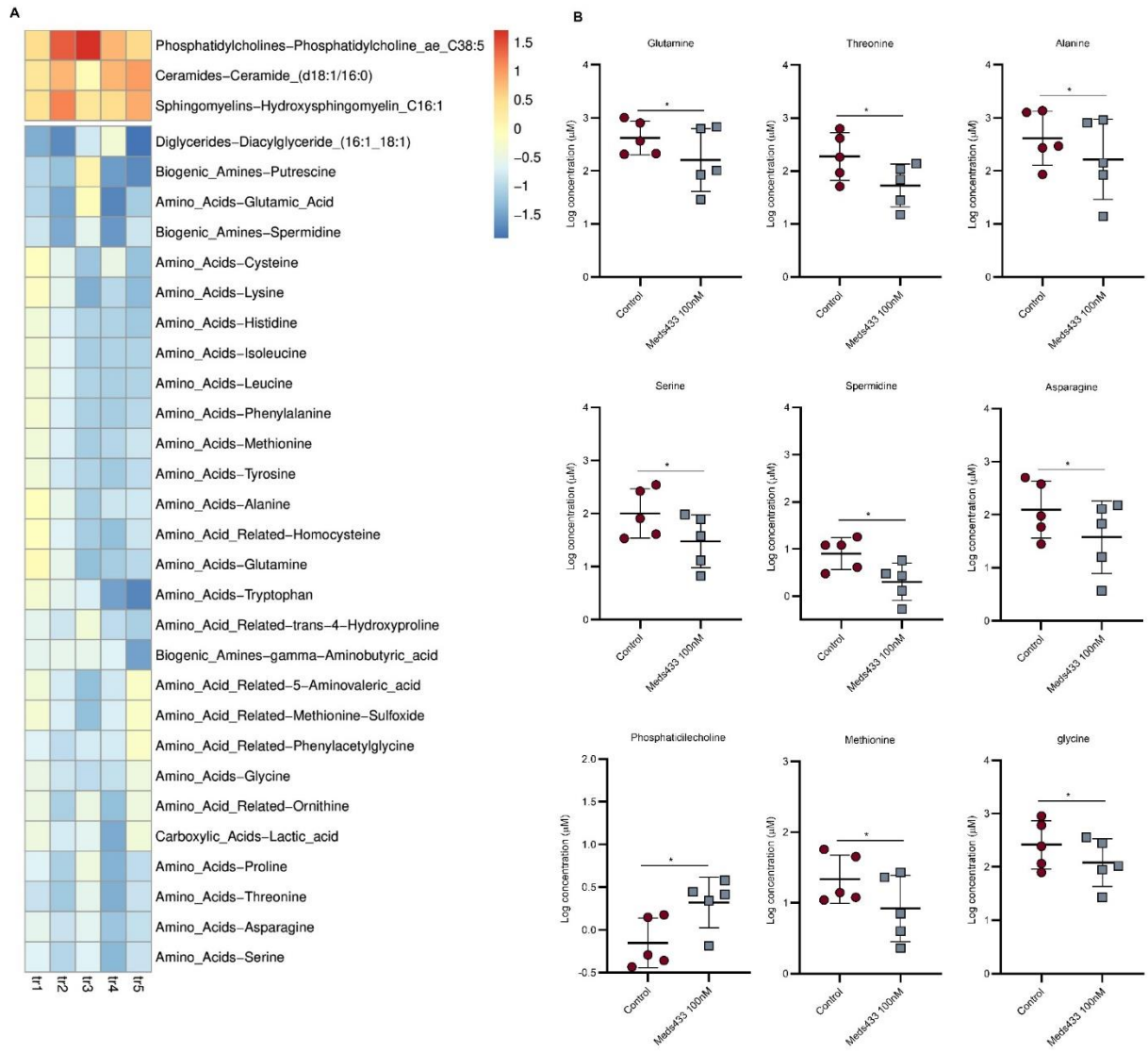

Figure 5. DHODH inhibition changes metabolic profile in CML CD34+. Altered metabolites following treatment of CML CD34+ (n:5) with Meds433 are displayed in (A). Also, the micromolar concentration of some metabolites in treated and untreated CML CD34+ is shown in (B). * p<0.05.

4.6- Meds433 suppresses tumor growth in the CML xenograft model

To demonstrate the efficacy of Meds433 in vivo we used a xenograft mouse model of a human cell line (KU-812). Two doses of Meds433 10mg/kg and 20mg/kg were

selected based on the maximum tolerated dose profile. Our results showed that administration of Meds433 10mg/kg and 20mg/kg significantly reduced tumor mass volume compared to the vehicle group (Fig. 6A). Also, reduction of the tumor weight was recorded in treated groups and confirmed the potency of Meds433 in controlling tumor growth (Fig. 6B). To analyze tumor burden in mice, human CD45 was measured in the peripheral blood, spleen and bone marrow. Based on our results we could not detect any tumor burden in peripheral blood (data not shown), while a small population of leukemic cells was detectable in the bone marrow and spleen. Tumor burden was reduced significantly in mice treated with Meds433 20mg/kg (Fig. 6C). Tumor morphology is shown in Fig. 6D and demonstrates the reduction of tumor size in treated mice compared to the vehicle (H&E staining of tumors is displayed in Supplemental Figure 2). One mice in the vehicle group had to be sacrificed due to high tumor volume. Also, in two mice treated with 20mg/kg of DHODH inhibitor, tumors were not detectable. These results prove the efficacy of DHODH inhibition in controlling CML cell growth in vivo. Also, at the end of the experiments, drug concentration and drug metabolites were measured in plasma of Meds433 10mg/kg and 20mg/kg treated mice (Fig. 6E).

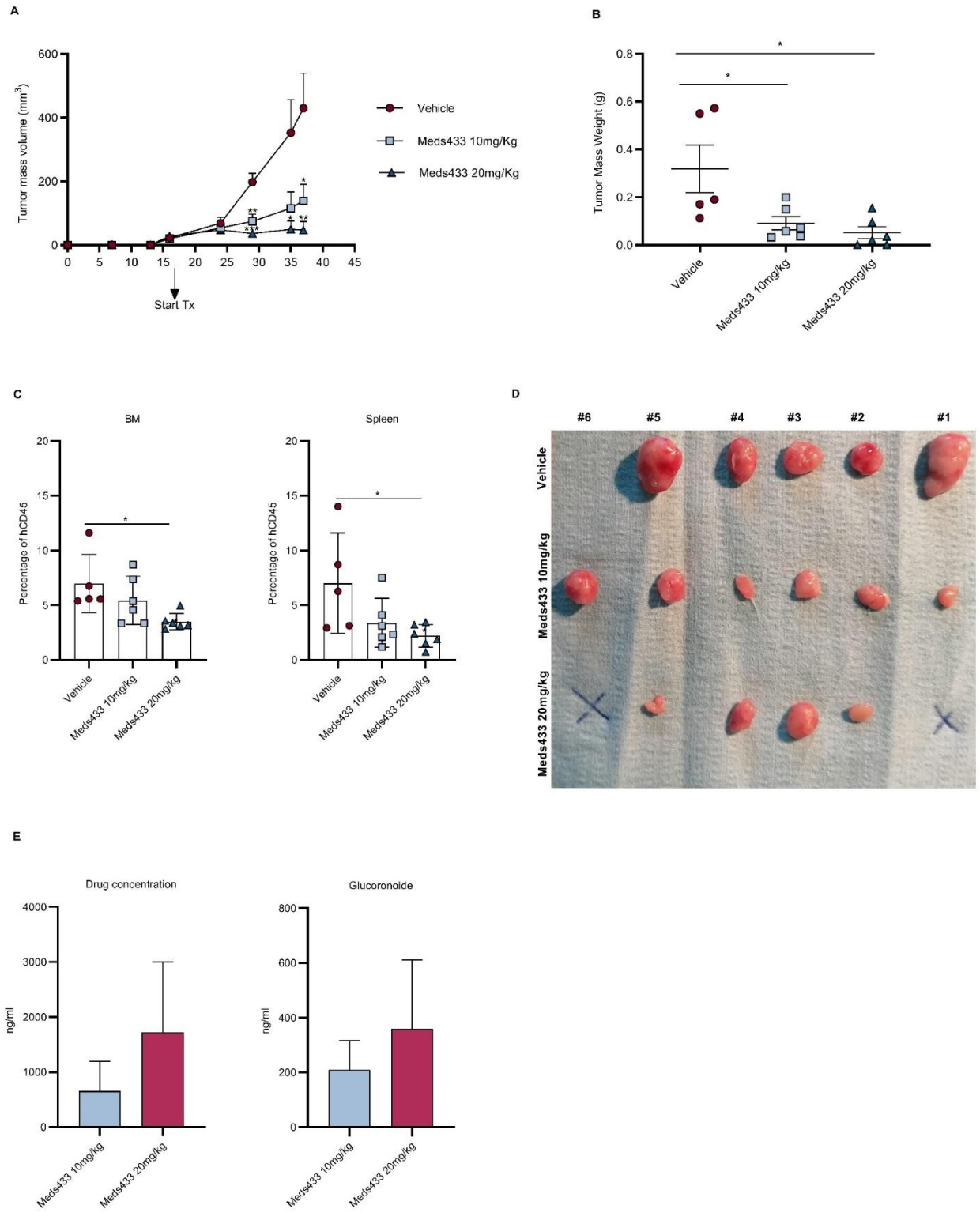

Figure 6. Meds433 impedes tumor growth in xenograft mice. Treatment of mice with 10mg/kg and 20mg/kg of Meds433 reduces tumor volume (A) and tumor weight (B). Also, a reduction in tumor burden after the treatment with Meds433 20mg/kg in BM and spleen is shown in (C). (D) represents size of tumors treated with Meds433. Noteworthy, the administration of Meds433 20mg/kg eliminated tumors

in two mice. Drug concentration and Glucoronoide as the drug metabolite in the plasma of treated mice are shown in (E). * $p<0.05$, ** $p<0.01$, *** $p<0.001$.

5- Discussion

Attempting TFR is considered as the standard of care and as the main goal of therapy in CML patients. About 40-50% of the newly diagnosed CML patients are eligible to stop TKIs, though half of them will relapse after a while. Although the focus of the therapy is on targeting BCR/ABL tyrosine kinase activity, it is worth mentioning that BCR/ABL transcript is also detectable in some healthy people. This might confirm that BCR/ABL should be present in a cell that has the biological potential to cause leukemia. So instead of focusing on BCR/ABL, targeting these biological differences between normal and leukemic cells might boost the number of patients attaining TFR (63-65). One of these differences between normal and leukemic cells is relevant to the metabolic reprogramming in leukemic cells that provides enough nucleotides and amino acids for their progression (66). DHODH is a key enzyme in pyrimidine biosynthesis and is a potential target for cancer treatment. In this study Meds433, as a potent DHODH inhibitor, was used to demonstrate the effect of pyrimidine deprivation in targeting CML stem/progenitor cells.

Previously it has been reported that inhibition of DHODH in different hematological malignancies such as AML, acute lymphoblastic leukemia, lymphoma, and myelodysplastic syndrome induces apoptosis and differentiation of the targeted cells (54-57, 67, 68). The predominance of each mechanism might be context-dependent or it might be related to the potency of a DHODH inhibitor. Our results demonstrated that blocking the pyrimidine biosynthesis pathway in CML CD34+ of newly diagnosed and resistant patients induces apoptosis. It seems there is a direct relation between nucleotide deprivation and activation of apoptosis in CML. This also proves the activity of the *de novo* pyrimidine biosynthesis in CML cells and their high demands for

nucleotides. It has been shown that pyrimidine deprivation results in upregulation of P53 and its stabilization as a tumor suppressor (69, 70). Also, ribosomal stress caused by DHODH inhibition plays a part in P53 activation (71, 72). As it is clear, DHODH inhibition significantly suppressed CML cell growth *in vitro* and *in vivo* and induced G2/M arrest. Based on the RNA seq data, this effect might be mediated through the reduction of a proto-oncogene such as MYC and upregulation of tumor suppressors such as P53 and DDIT3. Previous findings claimed that upregulation of P53 and downregulation of MYC, suppress cell growth, and induce cell cycle arrest (73). This inhibitory effect becomes more prominent when tumors in two xenograft mice treated with Meds433 20mg/kg could not be detectable. Apart from the role of MYC in apoptosis and proliferation, it also regulates cell metabolism through direct upregulation of DHODH and an increase in glutamine transporter (74-76). While glutamine is necessary for the *de novo* pyrimidine biosynthesis pathway our study showed that DHODH inhibition leads to the reduction of most amino acids including glutamine. This depletion might happen directly through the detrimental effect of DHODH inhibition on amino acids transporters, amino acids synthesis pathways, or indirectly via reduction of MYC. It looks like targeting DHODH activity in CML destroys all the building blocks for the progression of leukemic cells and induces significant metabolic stress in cells. This metabolic stress results from amino acid deprivation simultaneously activate P53 and cause cell cycle arrest (53, 77, 78). Furthermore, Amino acids such as glutamate, glycine, and cysteine are necessary for the synthesis of glutathione and maintenance of redox balance (79). This disruption in redox balance increases ROS production and decreases mitochondria membrane potential like what we saw in treated CML CD34+ (80). Also, reduction of erythroid lineage after the treatment with Meds433 might suggest the role of DHODH in erythropoiesis. It has

been reported that nucleotide production by glutamine has an essential role in erythroid lineage commitment, and a disruption in this pathway shifts the hematopoietic stem cells toward myelomonocytic lineage (81). Reduction of Erythroid genes and erythroid colonies after the treatment with Meds433 suggests the essential role of nucleotides in cell fate decisions. Moreover, the inflammatory profile caused by DHODH inhibition has a negative impact on the erythroid commitment (82) and promotes myelomonocytic differentiation. So, this metabolic stress might be the reason why leukemic cells differentiate to a specific lineage upon DHODH inhibition.

On balance, our study shows that the de novo pyrimidine biosynthesis pathway is active in CML cells which makes them vulnerable to its inhibition. Meds433 as a potent DHODH inhibitor depletes nucleotides production that leads to activation of apoptotic pathways, amino acids deprivation, and induction of metabolic stress in leukemic cells. This strategy might help us selectively target leukemic cells and to help more CML patients discontinue the therapy and to have a long-lasting remission.

6- References

1. Goldman JM. Chronic myeloid leukemia: a historical perspective. Semin Hematol. 2010;47(4):302-11.

2. Jabbour E, Kantarjian H. Chronic myeloid leukemia: 2020 update on diagnosis, therapy and monitoring. Am J Hematol. 2020;95(6):691-709.

3. Buchdunger E, Zimmermann J, Mett H, Meyer T, Muller M, Druker BJ, et al. Inhibition of the Abl protein-tyrosine kinase in vitro and in vivo by a 2-phenylaminopyrimidine derivative. Cancer Res. 1996;56(1):100-4.

4. Bixby D, Talpaz M. Seeking the causes and solutions to imatinib-resistance in chronic myeloid leukemia. Leukemia. 2011;25(1):7-22.

5. O'Hare T, Walters DK, Stoffregen EP, Jia T, Manley PW, Mestan J, et al. In vitro activity of Bcr-Abl inhibitors AMN107 and BMS-354825 against clinically relevant imatinib-resistant Abl kinase domain mutants. Cancer Res. 2005;65(11):4500-5.

6. Saglio G, Kim DW, Issaragrisil S, le Coutre P, Etienne G, Lobo C, et al. Nilotinib versus imatinib for newly diagnosed chronic myeloid leukemia. N Engl J Med. 2010;362(24):2251-9.

7. Shah NP, Tran C, Lee FY, Chen P, Norris D, Sawyers CL. Overriding imatinib resistance with a novel ABL kinase inhibitor. Science. 2004;305(5682):399-401.

8. Donato NJ, Wu JY, Stapley J, Gallick G, Lin H, Arlinghaus R, et al. BCR-ABL independence and LYN kinase overexpression in chronic myelogenous leukemia cells selected for resistance to STI571. Blood. 2003;101(2):690-8.

9. Kantarjian H, Shah NP, Hochhaus A, Cortes J, Shah S, Ayala M, et al. Dasatinib versus imatinib in newly diagnosed chronic-phase chronic myeloid leukemia. N Engl J Med. 2010;362(24):2260-70.

10. Cortes JE, Saglio G, Kantarjian HM, Baccarani M, Mayer J, Boque C, et al. Final 5-Year Study Results of DASISION: The Dasatinib Versus Imatinib Study in Treatment-Naive Chronic Myeloid Leukemia Patients Trial. J Clin Oncol. 2016;34(20):2333-40.

11. Boschelli DH, Ye F, Wang YD, Dutia M, Johnson SL, Wu B, et al. Optimization of 4-phenylamino-3-quinolinecarbonitriles as potent inhibitors of Src kinase activity. J Med Chem. 2001;44(23):3965-77.

12. Manley PW, Cowan-Jacob SW, Mestan J. Advances in the structural biology, design and clinical development of Bcr-Abl kinase inhibitors for the treatment of chronic myeloid leukaemia. Biochim Biophys Acta. 2005;1754(1-2):3-13.

13. Cortes JE, Gambacorti-Passerini C, Deininger MW, Mauro MJ, Chuah C, Kim DW, et al. Bosutinib Versus Imatinib for Newly Diagnosed Chronic Myeloid Leukemia: Results From the Randomized BFORE Trial. J Clin Oncol. 2018;36(3):231-7.

14. Gorre ME, Mohammed M, Ellwood K, Hsu N, Paquette R, Rao PN, et al. Clinical resistance to STI-571 cancer therapy caused by BCR-ABL gene mutation or amplification. Science. 2001;293(5531):876-80.

15. Lipton JH, Chuah C, Guerci-Bresler A, Rosti G, Simpson D, Assouline S, et al. Ponatinib versus imatinib for newly diagnosed chronic myeloid leukaemia: an international, randomised, open-label, phase 3 trial. Lancet Oncol. 2016;17(5):612-21.

16. Cortes JE, Kim DW, Pinilla-Ibarz J, le Coutre PD, Paquette R, Chuah C, et al. Ponatinib efficacy and safety in Philadelphia chromosome-positive leukemia: final 5-year results of the phase 2 PACE trial. Blood. 2018;132(4):393-404.

17. Claudiani S, Apperley JF, Khan A, Khorashad J, Milojkovic D. Prolonged treatment-free remission in chronic myeloid leukemia patients with previous BCR-ABL1 kinase domain mutations. Haematologica. 2020;105(5):e225-e7.

18. Stagno F, Breccia M, Di Raimondo F. On the road to treatment-free remission in chronic myeloid leukemia: what about 'the others'? Expert Rev Anticancer Ther. 2020;20(12):1075-81.

19. Mahon FX. Treatment-free remission in CML: who, how, and why? Hematology Am Soc Hematol Educ Program. 2017;2017(1):102-9.

20. Patel AB, O'Hare T, Deininger MW. Mechanisms of Resistance to ABL Kinase Inhibition in Chronic Myeloid Leukemia and the Development of Next Generation ABL Kinase Inhibitors. Hematol Oncol Clin North Am. 2017;31(4):589-612.

21. Milojkovic D, Apperley J. Mechanisms of Resistance to Imatinib and Second-Generation Tyrosine Inhibitors in Chronic Myeloid Leukemia. Clin Cancer Res. 2009;15(24):7519-27.

22. Zhao C, Blum J, Chen A, Kwon HY, Jung SH, Cook JM, et al. Loss of beta-catenin impairs the renewal of normal and CML stem cells in vivo. Cancer Cell. 2007;12(6):528-41.

23. Jamieson CH, Ailles LE, Dylla SJ, Muijtjens M, Jones C, Zehnder JL, et al. Granulocyte-macrophage progenitors as candidate leukemic stem cells in blast-crisis CML. N Engl J Med. 2004;351(7):657-67.

24. Coluccia AM, Vacca A, Dunach M, Mologni L, Redaelli S, Bustos VH, et al. Bcr-Abl stabilizes beta-catenin in chronic myeloid leukemia through its tyrosine phosphorylation. EMBO J. 2007;26(5):1456-66.

25. Riether C, Schurch CM, Flury C, Hinterbrandner M, Druck L, Huguenin AL, et al. Tyrosine kinase inhibitor-induced CD70 expression mediates drug resistance in leukemia stem cells by activating Wnt signaling. Sci Transl Med. 2015;7(298):298ra119.

26. Zhang B, Li M, McDonald T, Holyoake TL, Moon RT, Campana D, et al. Microenvironmental protection of CML stem and progenitor cells from tyrosine kinase inhibitors through N-cadherin and Wnt-beta-catenin signaling. Blood. 2013;121(10):1824-38.

27. Liu N, Zang S, Liu Y, Wang Y, Li W, Liu Q, et al. FZD7 regulates BMSCs-mediated protection of CML cells. Oncotarget. 2016;7(5):6175-87.

28. Gregory MA, Phang TL, Neviani P, Alvarez-Calderon F, Eide CA, O'Hare T, et al. Wnt/Ca2+/NFAT signaling maintains survival of Ph+ leukemia cells upon inhibition of Bcr-Abl. Cancer Cell. 2010;18(1):74-87.

29. Hanna A, Shevde LA. Hedgehog signaling: modulation of cancer properies and tumor mircroenvironment. Mol Cancer. 2016;15:24.

30. Dierks C, Beigi R, Guo GR, Zirlik K, Stegert MR, Manley P, et al. Expansion of Bcr-Abl-positive leukemic stem cells is dependent on Hedgehog pathway activation. Cancer Cell. 2008;14(3):238-49.

31. Sadarangani A, Pineda G, Lennon KM, Chun HJ, Shih A, Schairer AE, et al. GLI2 inhibition abrogates human leukemia stem cell dormancy. J Transl Med. 2015;13:98.

32. Zhao C, Chen A, Jamieson CH, Fereshteh M, Abrahamsson A, Blum J, et al. Hedgehog signaling is essential for maintenance of cancer stem cells in myeloid leukaemia. Nature. 2009;458(7239):776-9.

33. Diaz-Blanco E, Bruns I, Neumann F, Fischer JC, Graef T, Rosskopf M, et al. Molecular signature of CD34(+) hematopoietic stem and progenitor cells of patients with CML in chronic phase. Leukemia. 2007;21(3):494-504.

34. Cokic VP, Mojsilovic S, Jaukovic A, Kraguljac-Kurtovic N, Mojsilovic S, Sefer D, et al. Gene expression profile of circulating CD34(+) cells and granulocytes in chronic myeloid leukemia. Blood Cells Mol Dis. 2015;55(4):373-81.

35. Pellicano F, Scott MT, Helgason GV, Hopcroft LE, Allan EK, Aspinall-O'Dea M, et al. The antiproliferative activity of kinase inhibitors in chronic myeloid leukemia cells is mediated by FOXO transcription factors. Stem Cells. 2014;32(9):2324-37.

36. Xie S, Wang Y, Liu J, Sun T, Wilson MB, Smithgall TE, et al. Involvement of Jak2 tyrosine phosphorylation in Bcr-Abl transformation. Oncogene. 2001;20(43):6188-95.

37. Samanta A, Perazzona B, Chakraborty S, Sun X, Modi H, Bhatia R, et al. Janus kinase 2 regulates Bcr-Abl signaling in chronic myeloid leukemia. Leukemia. 2011;25(3):463-72.

38. Madapura HS, Nagy N, Ujvari D, Kallas T, Krohnke MCL, Amu S, et al. Interferon gamma is a STAT1-dependent direct inducer of BCL6 expression in imatinib-treated chronic myeloid leukemia cells. Oncogene. 2017;36(32):4619-28.

39. Gallipoli P, Cook A, Rhodes S, Hopcroft L, Wheadon H, Whetton AD, et al. JAK2/STAT5 inhibition by nilotinib with ruxolitinib contributes to the elimination of CML CD34+ cells in vitro and in vivo. Blood. 2014;124(9):1492-501.

40. Wilson A, Trumpp A. Bone-marrow haematopoietic-stem-cell niches. Nat Rev Immunol. 2006;6(2):93-106.

41. Jin L, Tabe Y, Konoplev S, Xu Y, Leysath CE, Lu H, et al. CXCR4 up-regulation by imatinib induces chronic myelogenous leukemia (CML) cell migration to bone marrow stroma and promotes survival of quiescent CML cells. Mol Cancer Ther. 2008;7(1):48-58.

42. Weisberg E, Azab AK, Manley PW, Kung AL, Christie AL, Bronson R, et al. Inhibition of CXCR4 in CML cells disrupts their interaction with the bone marrow microenvironment and sensitizes them to nilotinib. Leukemia. 2012;26(5):985-90.

43. Bhatia R, McCarthy JB, Verfaillie CM. Interferon-alpha restores normal beta 1 integrin-mediated inhibition of hematopoietic progenitor proliferation by the marrow microenvironment in chronic myelogenous leukemia. Blood. 1996;87(9):3883-91.

44. Krause DS, Lazarides K, Lewis JB, von Andrian UH, Van Etten RA. Selectins and their ligands are required for homing and engraftment of BCR-ABL1+ leukemic stem cells in the bone marrow niche. Blood. 2014;123(9):1361-71.

45. Corrado C, Saieva L, Raimondo S, Santoro A, De Leo G, Alessandro R. Chronic myelogenous leukaemia exosomes modulate bone marrow microenvironment through activation of epidermal growth factor receptor. J Cell Mol Med. 2016;20(10):1829-39.

46. Wang RN, Green J, Wang Z, Deng Y, Qiao M, Peabody M, et al. Bone Morphogenetic Protein (BMP) signaling in development and human diseases. Genes Dis. 2014;1(1):87-105.

47. Grockowiak E, Laperrousaz B, Jeanpierre S, Voeltzel T, Guyot B, Gobert S, et al. Immature CML cells implement a BMP autocrine loop to escape TKI treatment. Blood. 2017;130(26):2860-71.

48. Zhang B, Nguyen LXT, Li L, Zhao D, Kumar B, Wu H, et al. Bone marrow niche trafficking of miR-126 controls the self-renewal of leukemia stem cells in chronic myelogenous leukemia. Nat Med. 2018;24(4):450-62.

49. Traer E, Javidi-Sharifi N, Agarwal A, Dunlap J, English I, Martinez J, et al. Ponatinib overcomes FGF2-mediated resistance in CML patients without kinase domain mutations. Blood. 2014;123(10):1516-24.

50. Bourgeais J, Ishac N, Medrzycki M, Brachet-Botineau M, Desbourdes L, Gouilleux-Gruart V, et al. Oncogenic STAT5 signaling promotes oxidative stress in chronic myeloid leukemia cells by repressing antioxidant defenses. Oncotarget. 2017;8(26):41876-89.

51. Baccarani M, Gale RP. Why chronic myeloid leukaemia cannot be cured by tyrosine kinase-inhibitors. Leukemia. 2021;35(8):2199-204.

52. Zhou Y, Tao L, Zhou X, Zuo Z, Gong J, Liu X, et al. DHODH and cancer: promising prospects to be explored. Cancer Metab. 2021;9(1):22.

53. Madak JT, Bankhead A, 3rd, Cuthbertson CR, Showalter HD, Neamati N. Revisiting the role of dihydroorotate dehydrogenase as a therapeutic target for cancer. Pharmacol Ther. 2019;195:111-31.

54. McDonald G, Chubukov V, Coco J, Truskowski K, Narayanaswamy R, Choe S, et al. Selective Vulnerability to Pyrimidine Starvation in Hematologic Malignancies Revealed by AG-636, a Novel Clinical-Stage Inhibitor of Dihydroorotate Dehydrogenase. Mol Cancer Ther. 2020;19(12):2502-15.

55. Christian S, Merz C, Evans L, Gradl S, Seidel H, Friberg A, et al. The novel dihydroorotate dehydrogenase (DHODH) inhibitor BAY 2402234 triggers differentiation and is effective in the treatment of myeloid malignancies. Leukemia. 2019;33(10):2403-15.

56. Gaidano V, Houshmand M, Vitale N, Carra G, Morotti A, Tenace V, et al. The Synergism between DHODH Inhibitors and Dipyridamole Leads to Metabolic Lethality in Acute Myeloid Leukemia. Cancers (Basel). 2021;13(5).

57. Kayamori K, Nagai Y, Zhong C, Kaito S, Shinoda D, Koide S, et al. DHODH inhibition synergizes with DNA-demethylating agents in the treatment of myelodysplastic syndromes. Blood Adv. 2021;5(2):438-50.

58. Sykes DB, Kfoury YS, Mercier FE, Wawer MJ, Law JM, Haynes MK, et al. Inhibition of Dihydroorotate Dehydrogenase Overcomes Differentiation Blockade in Acute Myeloid Leukemia. Cell. 2016;167(1):171-86 e15.

59. Dobin A, Davis CA, Schlesinger F, Drenkow J, Zaleski C, Jha S, et al. STAR: ultrafast universal RNA-seq aligner. Bioinformatics. 2013;29(1):15-21.

60. Liao Y, Smyth GK, Shi W. featureCounts: an efficient general purpose program for assigning sequence reads to genomic features. Bioinformatics. 2014;30(7):923-30.

61. Robinson MD, McCarthy DJ, Smyth GK. edgeR: a Bioconductor package for differential expression analysis of digital gene expression data. Bioinformatics. 2010;26(1):139-40.

62. Dieterle F, Ross A, Schlotterbeck G, Senn H. Probabilistic quotient normalization as robust method to account for dilution of complex biological mixtures. Application in 1H NMR metabonomics. Anal Chem. 2006;78(13):4281-90.

63. Gale RP, Apperley JF. Transmission of CML or of t(9; 22) and BCR/ABL? They are not the same. Bone Marrow Transplant. 2015;50(12):1582.

64. Baccarani M, Gale RP. Why chronic myeloid leukaemia cannot be cured by tyrosine kinase-inhibitors. Leukemia. 2021.

65. Ismail SI, Naffa RG, Yousef AM, Ghanim MT. Incidence of bcrabl fusion transcripts in healthy individuals. Mol Med Rep. 2014;9(4):1271-6.

66. Castro I, Sampaio-Marques B, Ludovico P. Targeting Metabolic Reprogramming in Acute Myeloid Leukemia. Cells. 2019;8(9).

67. Zhou J, Yiying Quah J, Ng Y, Chooi JY, Hui-Min Toh S, Lin B, et al. ASLAN003, a potent dihydroorotate dehydrogenase inhibitor for differentiation of acute myeloid leukemia. Haematologica. 2020;105(9):2286-97.

68. Cao L, Weetall M, Trotta C, Cintron K, Ma J, Kim MJ, et al. Targeting of Hematologic Malignancies with PTC299, A Novel Potent Inhibitor of Dihydroorotate Dehydrogenase with Favorable Pharmaceutical Properties. Mol Cancer Ther. 2019;18(1):3-16.

69. Ladds M, van Leeuwen IMM, Drummond CJ, Chu S, Healy AR, Popova G, et al. A DHODH inhibitor increases p53 synthesis and enhances tumor cell killing by p53 degradation blockage. Nat Commun. 2018;9(1):1107.

70. Khutornenko AA, Roudko VV, Chernyak BV, Vartapetian AB, Chumakov PM, Evstafieva AG. Pyrimidine biosynthesis links mitochondrial respiration to the p53 pathway. Proc Natl Acad Sci U S A. 2010;107(29):12828-33.

71. Lafita-Navarro MC, Venkateswaran N, Kilgore JA, Kanji S, Han J, Barnes S, et al. Inhibition of the de novo pyrimidine biosynthesis pathway limits ribosomal RNA transcription causing nucleolar stress in glioblastoma cells. PLoS Genet. 2020;16(11):e1009117.

72. Hubackova S, Davidova E, Boukalova S, Kovarova J, Bajzikova M, Coelho A, et al. Replication and ribosomal stress induced by targeting pyrimidine synthesis and cellular checkpoints suppress p53-deficient tumors. Cell Death Dis. 2020;11(2):110.

73. Dorasamy MS, Choudhary B, Nellore K, Subramanya H, Wong PF. Dihydroorotate dehydrogenase Inhibitors Target c-Myc and Arrest Melanoma, Myeloma and Lymphoma cells at S-phase. J Cancer. 2017;8(15):3086-98.

74. Dang CV. MYC on the path to cancer. Cell. 2012;149(1):22-35.

75. Liu YC, Li F, Handler J, Huang CR, Xiang Y, Neretti N, et al. Global regulation of nucleotide biosynthetic genes by c-Myc. PLoS One. 2008;3(7):e2722.

76. Chen H, Liu H, Qing G. Targeting oncogenic Myc as a strategy for cancer treatment. Signal Transduct Target Ther. 2018;3:5.

77. Tajan M, Hock AK, Blagih J, Robertson NA, Labuschagne CF, Kruiswijk F, et al. A Role for p53 in the Adaptation to Glutamine Starvation through the Expression of SLC1A3. Cell Metab. 2018;28(5):721-36 e6.

78. Gaglio D, Soldati C, Vanoni M, Alberghina L, Chiaradonna F. Glutamine deprivation induces abortive s-phase rescued by deoxyribonucleotides in k-ras transformed fibroblasts. PLoS One. 2009;4(3):e4715.

79. Lu SC. Glutathione synthesis. Biochim Biophys Acta. 2013;1830(5):3143-53.

80. Lieu EL, Nguyen T, Rhyne S, Kim J. Amino acids in cancer. Exp Mol Med. 2020;52(1):15-30.

81. Oburoglu L, Tardito S, Fritz V, de Barros SC, Merida P, Craveiro M, et al. Glucose and glutamine metabolism regulate human hematopoietic stem cell lineage specification. Cell Stem Cell. 2014;15(2):169-84.

82. Mei Y, Zhao B, Basiorka AA, Yang J, Cao L, Zhang J, et al. Age-related inflammatory bone marrow microenvironment induces ineffective erythropoiesis mimicking del(5q) MDS. Leukemia. 2018;32(4):1023-33.